

Star Formation History in Early-Type Galaxies.

I. The Line Absorption Indices Diagnostics

Rosaria Tantalò & Cesare Chiosi

Department of Astronomy, University of Padova, Vicolo dell'Osservatorio 2, 35122 Padova, Italy
E-mail: tantalo@pd.astro.it; chiosi@pd.astro.it

Submitted: November 2003; Revised: April 2004

ABSTRACT

To unravel the formation mechanism and the evolutionary history of Elliptical Galaxies (EGs) is one of the goals of modern astrophysics. In a simplified picture of the issue, the question to be answered is whether they have formed by hierarchical merging of pre-existing sub-structures (maybe disc galaxies) made of stars and gas, each merging event likely accompanied by strong star formation, or conversely, they originated from the early aggregation of lumps of gas turned into stars in the remote past via a burst-like episode ever since followed by quiescence so as to mimic a sort of monolithic process. Even if the two alternatives seem to oppose each other, actually they may concur to shaping the final properties of EG's as seen today. Are there distinct signatures of the underlying dominant process in the observational data? To this aim we have examined the line absorption indices on the Lick system of the normal, field EGs of Trager (1997) and the interacting EGs (pair- and shell-objects) of Longhetti et al. (2000). The data show that both normal, field and interacting galaxies have the same scattered but smooth distribution in the H_β vs. $[\text{MgFe}]$ plane even if the interacting ones show a more pronounced tail toward high H_β values. This may suggest that a common physical cause is at the origin of their distribution. There are two straightforward interpretations of increasing complexity: (1) EGs span true large ranges of ages and metallicities. The age youth is the signature of the aggregation mechanism, each event accompanied by metal enrichment. This simple scheme cannot, however, explain other spectro-photometric properties of EGs and has to be discarded. (2) The bulk population of stars is old but subsequent episodes of star formation scatter the EGs in the diagnostic planes. However, this scheme would predict an outstanding clump at low H_β values, contrary to what is observed. The model can be cured by supposing that the primary star formation activity lasted for a significant fraction of the Hubble time ($5 \text{ Gyr} \leq T \leq 13 \text{ Gyr}$) accompanied by global metal enrichment. The “younger” galaxies are more metal-rich. The later burst of star formation should be small otherwise too many high H_β objects would be observed. Therefore, the distribution of normal, pair- and shell-galaxies in the H_β vs. $[\text{MgFe}]$ plane is due to the global metal enrichment. Even though the above schemes provide a formal explanation, they seem to be too demanding because of the many *ad hoc* ingredients that have to be introduced. Furthermore they neglect the observationally grounded hint that the stellar content of EGs is likely enhanced in α -elements with $[\alpha/Fe]$ ranging from 0.1 to 0.4 dex. We propose here a new scheme, in which the bulk dispersion of galaxies in the H_β vs. $[\text{MgFe}]$ plane is caused by a different mean degree of enhancement. In this model, neither large age ranges nor universal enrichment law for the old component are required and the observed distribution along H_β is naturally recovered. Furthermore, later bursts of stellar activity are a rare event interesting only those galaxies with very high H_β (roughly > 2.5). Finally, simulations of the scatter in broad-band colors of EG's seem to confirm that the bulk stars have formed in the remote past, and that mergers and companion star formation in a recent past are not likely, unless the intensity of the secondary activity is very small.

Key words: galaxies: elliptical – galaxies: evolution – galaxies: formation – galaxies: abundances

arXiv:astro-ph/0405540v1 27 May 2004

1 INTRODUCTION

Determining the age of the bulk stellar content of Elliptical Galaxies (EGs) is basic to reconstructing the past history of star formation and to setting clues on the galaxy formation process itself. Two competing scenarios are proposed: the monolithic picture in which a single dominant episode of star formation occurred in the past, ever since followed by quiescence and passive evolution (secondary episodes are however always possible); the hierarchical scheme, in which a series of mergers of smaller sub-units has taken place over the billions of years, each of those likely accompanied by star forming activity (mergers of inert objects with no additional star formation cannot be excluded). Current ideas concerning the two competing pictures of galaxy formation have been critically reviewed by Ellis (1998) and Peebles (2002). In short the present day view of structure formation suggests that roughly half of the large EGs were assembled at $z < 1$. However, observational evidence of variations with redshift of the color-magnitude, fundamental plane, size-magnitude, K-magnitude-redshift relations indicate that large EGs have already formed in the distant past at $z \geq 2$.

In order to discriminate between the two schemes, the key question to be addressed and hopefully answered is what kind of signatures the stellar populations of a galaxy have inherited from the forming mechanism. The diagnostic to our disposal is mainly based on magnitudes, colors, integrated spectra, luminosity weighed line strength indices, estimates of chemical abundances and abundance ratios together with the spatial gradients in those quantities. As for the line absorption indices, gradients in Mg_2 and $\langle Fe \rangle$ (and others) observed in EGs (Worthey 1992; González 1993; Davies et al. 1993; Carollo et al. 1993; Carollo & Danziger 1994a,b; Balcells & Peletier 1994; Fisher et al. 1995; Carrasco et al. 1995; Fisher et al. 1996) have often been interpreted as indicating that the abundances of α -elements (Mg, O, etc.) with respect to iron are enhanced – $[\alpha/Fe] > 0$ – in the central regions. Opposite conclusions however exist (Kuntschner 1998; Davies et al. 2001). Furthermore, limited to the nuclear regions, indices vary passing from one galaxy to another (González 1993; Trager et al. 2000b,a). Looking at the correlation between Mg_2 and $\langle Fe \rangle$ (or similar indices) for the galaxies in those samples, Mg_2 increases faster than $\langle Fe \rangle$, which is once more interpreted as due to enhancement of α -elements in some galaxies. In addition to this, since the classical paper by Burstein et al. (1988), the index Mg_2 is known to increase with the velocity dispersion (and hence mass and luminosity) of the galaxy. Standing on this body of data the conviction arose that the degree of enhancement in α -elements ought to increase passing from dwarf to massive EGs (Faber et al. 1992; Worthey et al. 1994; Matteucci 1994, 1997; Matteucci et al. 1998).

Another point to consider is whether normal and interacting galaxies (i.e. shell- and pair-objects) show any systematic difference in colors and line absorption indices. The subject was addressed by Longhetti et al. (1998a,b, 1999, 2000), whose results will be shortly summarized below.

Using this body of data, can we infer the age, the metallicity and the degree of enhancement for the bulk stars in an EG? The task is not trivial because age and metallicity have similar effects on the spectrum of a galaxy, i.e.

the spectrum and hence the colors of an old and metal-poor population may look like those of a young and metal-rich one, the so-called *age metallicity-degeneracy* pointed out long ago by Renzini & Buzzoni (1986). The degeneracy is also further complicated by effects both on the age and metallicity caused by the enhancement in α -elements. A promising way-out is perhaps offered by the system of line absorption indices introduced by the Lick group (Worthey 1992; Worthey et al. 1994, and reference therein) which have been extensively used to infer the age, metallicity, and abundance ratios of EGs (Bressan et al. 1996; Tantalo et al. 1998; Kuntschner & Davies 1998; Kuntschner 1998; Jørgensen 1999; Kuntschner 2000; Trager et al. 2000b,a; Kuntschner et al. 2001; Vazdekis et al. 2001; Davies et al. 2001; Poggianti et al. 2001; Maraston et al. 2003; Thomas et al. 2003a,b; Thomas & Maraston 2003; Tantalo & Chiosi 2004).

Let us shortly summarize the key steps of those articulated analysis, paying particular attention to the age for which often the conclusion that EGs show evidence of recent star formation either for the whole bulk stellar population or part it has been drawn. The age youth has often been taken as the signature of the hierarchical mechanism.

(i) Starting from the pioneering study of González (1993) of “normal galaxies” (i.e. those with no sign of dynamical interaction, accretion, etc.) in the local Universe, different groups analyzed the distribution of galaxies in the H_β vs. $[MgFe]$ diagnostic plane and others of the same kind (Buzzoni et al. 1992; Buzzoni et al. 1994; Bressan et al. 1996; Tantalo 1998; Tantalo et al. 1998) using the Single Stellar Populations (SSP) approximation, i.e. the stellar content of a galaxy is reduced to SSP of suitable age, metallicity and degree of enhancement. The index H_β is considered to be a good age indicator, whereas $[MgFe]$ is considered to be most sensitive to the metallicity. In reality both indices are sensitive to age, metallicity, and degree of enhancement (see also González 1993; Tantalo & Chiosi 2004, for similar remarks). Since EGs are more scattered in H_β than in $[MgFe]$ and do not follow the relation expected for coeval old objects matching the Color-Magnitude relation (Bower et al. 1992a,b), it was argued that H_β traces the age of the bulk stars, thus suggesting that some galaxies are truly young objects. However, a closer scrutiny of the problem led Bressan et al. (1996) to suggest all galaxies in that sample should be old but with different histories of star formation. Some of them completed their stellar activity in the far past with no evidence of subsequent episodes. Others had a more prolonged star forming history, perhaps in recurrent episodes of short duration. Looking at the galaxy to galaxy differences δH_β and $\delta[MgFe]$ in the nuclear values and their correlation with Σ_0 , the suggestion was advanced that the global duration of the star forming activity gets longer at decreasing Σ_0 (galaxy mass). This was later confirmed by dynamical Tree-SPH simulations of early type galaxies by Kawata (1999, 2001b,a) and Chiosi & Carraro (2002). In addition to this, Bressan et al. (1996) and Longhetti et al. (2000) tried to understand the effect brought to the indices of a population of old stars by a recent episode of star formation. The results is that indices like H_β are strongly affected by even small percentages of young stars: as long as star formation is active they jump to very high values and when star formation is over they fall back to the original value

on a time-scale of about 1 Gyr. Other indices like Mg_2 , $\langle Fe \rangle$ are much less affected even if the companion chemical enrichment may somewhat change them. In diagnostics planes like H_β vs. $\langle Fe \rangle$ the galaxy performs and extended loop elongated towards the H_β axis, thus causing an artificial dispersion which could be interpreted as an age dispersion, whereas what we are really seeing is the transient phase associated to the temporary stellar activity. Consequently, the idea that the dispersion in H_β measures the age of the last episode of star formation instead of the age of the bulk population was commonly accepted. Finally, EGs likely have mean metallicities in the range $Z_\odot \leq Z \leq 3Z_\odot$ as indicated by comparing theoretical models with data (see also Bressan et al. 1996; Greggio 1996).

(ii) Tantalo et al. (1998) examining the González galaxies, in order to infer from the simultaneous fit of H_β , Mg_2 , and $\langle Fe \rangle$ the age, the metallicity, and the enhancement factor $[\alpha/Fe]$, noticed that: (a) In a small group of galaxies, the nucleus appears to be more metal-rich, more α -enhanced, and younger (i.e. containing a significant fraction of young stars) than the external regions. (b) The galaxy to galaxy differences δH_β , δMg_2 , and $\delta \langle Fe \rangle$ for the nuclear regions yield age differences for the last episode of star formation perhaps correlating with the galaxy mass. In other words, while there seems to be a sort of *upper limit* to the age of the bulk stars, traced by quiescent galaxies (no signs of rejuvenation), it seems also that the last episode of star formation took place closer and closer to the present at decreasing galaxy luminosity (mass).

(iii) Surprisingly, in the H_β vs. $[MgFe]$ plane, shell-, pair-galaxies (i.e. those with signs of dynamical interactions) and normal galaxies share the same distribution (Longhetti et al. 2000). There is, however, a group of peculiar galaxies with much stronger H_β as compared to the normal ones. Does it mean that the scatter seen in this diagram has a common origin, perhaps secondary episodes of star formation that can occur independently of whether or not a galaxy is interacting? This will be discussed in detail in Section 5.3 below.

Thanks to these achievements, the H_β vs. $[MgFe]$ plane (and others of the same kind) for SSP of both solar and α -enhanced abundance ratios soon became a popular tool to estimate the age, metallicity and degree of enhancement of galaxies (Kuntschner & Davies 1998; Kuntschner 1998; Jørgensen 1999; Kuntschner 2000; Kuntschner et al. 2001; Vazdekis et al. 2001; Davies et al. 2001; Poggianti et al. 2001). The advent of large libraries of SSPs with different chemical compositions including the effect of different $[\alpha/Fe]$ ratios, e.g. Salasnich et al. (2000), on one hand spurred the construction of corresponding libraries of line absorption indices, on the other hand made the many-indices fitting technique (three at least) of general use (e.g. Trager et al. 2000b,a; Maraston et al. 2003; Thomas et al. 2003a,b; Thomas & Maraston 2003; Tantalo & Chiosi 2004) and introduced new techniques more sophisticated than the two-indices diagnostics. The solution for ages, metallicities and $[\alpha/Fe]$ ratios based on large samples of galaxies, e.g. the Trager (1997) list, once more yields large ranges of ages, metallicities, and abundance ratios, as amply discussed by Tantalo & Chiosi (2004).

Although we have repeatedly mentioned that the large spread in age formally assigned to galaxies (EGs in partic-

ular) on the base of the line absorption diagnostics has to be interpreted as referring to the last episode of star formation rather than the age of the bulk stellar population, quantifying the relative efficiency of the different star forming processes has still remained unsettled but for a few preliminary studies (Bressan et al. 1996; Longhetti et al. 2000). The question is: how much a recent, minute episode of star formation, engaging a small fraction of the total mass, may alter the indices of an otherwise old population of stars in EGs? In this paper we reconsider the whole problem at the light of recent developments in the observational data and theory of population synthesis concerning the theoretical line absorption indices in which the effect of $[\alpha/Fe]$ ratios are taken into account. We intend in particular to investigate the effect of different histories of star formation and chemical enrichment from galaxy to galaxy and to explore in more detail the effects of late bursts of stellar activity.

The paper is organized as follows. In Section 2 we shortly summarize the definition of line absorption indices and total enhancement parameter, mention the *Fitting Functions* in use, recall the main properties of stellar models and associated isochrones we have adopted to calculate SSPs and their integrated indices, and finally describe the key ingredients of the library of stellar spectra we have used to calculate indices and broad-band colors of SSPs. In Section 3 we describe the indices for SSPs at varying metallicity, enhancement parameter, and age. In Section 4 we present the technique to calculate the indices of composed objects made of at least two SSPs of different metallicity, enhancement, and age. In addition to this, we show the path in several two-indices-plane described by old galaxies rejuvenated by an episode of star formation of different intensity and age. In Section 5, we present the observational data we want to interpret, i.e. the Trager (1997) sample of normal galaxies complemented by the sample of Longhetti et al. (2000) for shell- and pair-galaxies. The analysis is based on the distribution of galaxies in the diagnostic plane H_β vs. $[MgFe]$. Three different interpretations are explored: (i) The bulk stellar population of early-type galaxies span large ranges of metallicities and ages. This is equivalent to say that galaxies can form over time interval comparable to the Hubble time. (ii) The bulk stellar population is very old (say 10-13 Gyr) in all galaxies but recent episodes of star formations (bursts) engaging a small fraction of the total mass are present in most of them. Both explanations can hardly fit the distribution of galaxies along the H_β direction unless *ad hoc* hypotheses are made for a sort of Universal Law of Metal Enrichment (ULME). Since severe drawbacks of these explanations are either the large range of ages together with the *ad hoc* hypothesis of ULME and/or the otherwise unavoidable existence of subsequent bursts of stellar activity in all galaxies, a third alternative is explored. (iii) The bulk population of stars in all galaxies is very old (once again 10-13 Gyr) but span large ranges of metallicity and global enhancement factor. This is equivalent to say that each galaxy has its own history of star formation determining the chemical properties. No ULME and no subsequent bursts of stellar activity are required to account for the observed distribution of the majority of galaxies. Only a few objects with unusually strong H_β are likely in the bursting mode. In Section 6, the last interpretation is critically discussed, the case of two template galaxies is examined in detail, and a few remarks

are made on the different range of H_β spanned by EGs in Coma and local vicinity. In Section 7 we address the question: how intense and old subsequent bursts of stellar activity ought to be without violating the constraint imposed by the present-day mean broad-band colors of EGs? Finally, in Section 8 we summarize the results and presents some concluding remarks.

2 THEORY OF LINE ABSORPTION INDICES

2.1 Definition

The technique to calculate line-strength indices of SSPs is amply described in Worthey et al. (1994); Bressan et al. (1996); Tantalo et al. (1998); Maraston et al. (2003) and Tantalo & Chiosi (2004). The reader is referred to those articles and references therein for a detailed description of the method. Here we limit ourselves to summarize a few basic points for the sake of clarity. Suffice here to recall that a line absorption index is constructed from the ratio F_l/F_c where F_l and F_c are the fluxes in the line and pseudo-continuum, respectively. The flux F_c is calculated by interpolating to the central wavelength of the absorption line, the fluxes in the midpoints of the red and blue pseudo-continua bracketing the line (Worthey et al. 1994).

2.2 Fitting Functions

Since the Lick system of indices (Burstein et al. 1984; Faber et al. 1985; Worthey et al. 1994) stands on a spectra library with fixed resolution of 8\AA , whereas most of the synthetic spectra in use have a different resolution, to overcome the difficulty, the so-called *Fitting Functions* (\mathcal{FF}) have been introduced. They express the indices measured on the observed spectra of a large number of stars with known gravity, T_{eff} , and chemical composition ($[\text{Fe}/\text{H}]$) as functions of these parameters (Worthey et al. 1994). In the following we adopt the Worthey (1992) \mathcal{FF} , extended however to high temperature stars ($T_{\text{eff}} \approx 10,000\text{ K}$) as reported in Longhetti et al. (1998a).

2.3 Integrated indices of SSPs

They are derived in the following way. A SSP is described by an isochrone in the HRD whose elemental bins (fixed by $\Delta \log L/L_\odot$ and $\Delta \log T_{\text{eff}}$) can be conceived as a “star” of suitable luminosity (gravity), T_{eff} and metallicity. Each elemental bin is in turn populated by a number N_i of such stars given by

$$N_i = \int_{m_a}^{m_b} \phi(m) dm \quad (1)$$

where m_a and m_b are the minimum and maximum star mass in the bin and $\phi(m)$ is the initial mass function in number. We start from the typical star of a bin for which we may derive the indices from the \mathcal{FF} . The indices are then inverted to derive the flux in the absorption line, $F_{l,i}^*$, and in the pseudo-continuum $F_{c,i}^*$. Known the index for a single star, we weigh its contribution to the integrated value on

the relative number of stars of the same type. We calculate the ratio

$$\frac{\sum_i F_{l,i}^* N_i}{\sum_i F_{c,i}^* N_i} \quad (2)$$

where N_i is the above number of stars in the generic bin, and finally insert the ratio into the definition of each index as appropriate.

2.4 α -enhanced chemical compositions

Total enhancement. To distinguish the enhancement of individual species from the *total one* characterizing a given chemical mixture, Tantalo & Chiosi (2004) introduce the parameter Γ defined as follows. Let us take a certain mixture of elements with mass abundances X_j of each species, and total metallicity Z (sum of the X_j for all elements heavier than He). The ratio of the mass abundance of an element with respect to Fe and to the Sun is given by

$$\left[\frac{X_j}{X_{Fe}} \right] = \log \left(\frac{X_j}{X_{Fe}} \right) - \log \left(\frac{X_j}{X_{Fe}} \right)_\odot \quad (3)$$

Let us now assume that the ratio $[X_j/X_{Fe}]$ of some elements is changed under the conditions that the abundance of Fe with respect to the Sun and the total metallicity Z remain constant. The mass-abundances of all species in the new mixture are accordingly scaled to a new value X'_j . The *total enhancement factor* Γ is

$$\Gamma = -\log \left(\frac{X'_{Fe}}{X_{Fe}^\odot} \right) \quad (4)$$

See Tantalo & Chiosi (2004) for all other details.

The Tripicco & Bell (1995) Response Functions. A method designed to include the effects of enhancement on line absorption indices has been suggested by Tripicco & Bell (1995, TB95), who introduce the concept of *Response Functions*. In brief from model atmospheres and spectra for three stars of assigned effective temperature and gravity, i.e. a Cool-Dwarf (CD), a Turn-Off (TO), and a Cool-Giant (CG), they calculate the absolute indices I_0 . Doubling the abundances X_i of the C, N, O, Mg, Fe, Ca, Na, Si, Cr, and Ti in steps of $\Delta[X_i/H]=0.3$ dex they determine the incremental ratios $\Delta I_0/\Delta[X_i/H]$ from which the *Response Function* $R_{0.3}(i)$ for any index corresponding to a variation of the element *i-th* $\Delta[X_i/H] = +0.3$ dex, can be derived

$$R_{0.3}(i) = \frac{1}{I_0} \frac{\Delta I_0}{\Delta[X_i/H]} 0.3$$

The *Response Functions* for the Cool-Dwarf, Turn-Off, and Cool-Giant stars constitute the milestones of the calibration.

The mathematical algorithm for correcting an index from solar to α -enhanced element partitions is taken from Trager et al. (2000b) and Tantalo & Chiosi (2004) to whom the reader should refer for all details. In brief, starting from the assumption that fractional variation of an index

Table 1. Chemical composition and [Fe/H] as function of Γ for the SSPs in use.

			$\Gamma = 0.$	$\Gamma = 0.3557$	$\Gamma = 0.50$
Z	Y	X	[Fe/H]	[Fe/H]	[Fe/H]
0.008	0.248	0.7440	-0.3972	-0.7529	-0.8972
0.019	0.273	0.7080	0.0000	-0.3557	-0.5000
0.040	0.320	0.6400	0.3672	0.0115	-0.1328
0.070	0.338	0.5430	0.6824	0.3267	0.1715

to changes of the chemical parameters is the same as that for the reference index I_0 , the following expression is derived

$$\frac{\Delta I}{I} = \frac{\Delta I_0}{I_0} = \left\{ \prod_i [1 + R_{0.3}(i)]^{\frac{[X_i/H]}{0.3}} \right\} - 1 \quad (5)$$

where $R_{0.3}(i)$ are the *Response Function* tabulated by TB95. Relation (5) can be applied under the obvious condition that $I/I_0 > 0$.

The above algorithm is used to evaluate the fractional variations for the three calibrators, i.e. $(\Delta I/I)_{CD}$, $(\Delta I/I)_{TO}$ and $(\Delta I/I)_{CG}$. Since in general a star or elemental bin along an isochrone will have effective temperature and gravity different from the ones of the three calibrators, and the fractional variations for these latter are also different, to evaluate the total fractional variation to be used for the particular star (isochrone bin) under examination, we linearly interpolate both in effective temperature and gravity among the fractional variations of the calibrators weighing their contribution according to their distance from the current star in the HR-Diagram. For a detailed discussion of this topic and associated uncertainties see Tantalò & Chiosi (2004).

2.5 Stellar models and isochrones

The SSP indices are based on the Padova Library of stellar models and companion isochrones according to the version by Girardi et al. (2000) and Girardi (2003, private communication). This particular set of stellar models/isochrones differs from the classical one by Bertelli et al. (1994) for the efficiency of convective overshooting and the prescription for the mass-loss rate along the Asymptotic Red Giant Branch (AGB) phase. For the reasons amply explained by Tantalò & Chiosi (2004), we prefer not to use the more recent stellar models by Salasnich et al. (2000) in which the effect of α -enhancement is already included in the stellar opacity. Since indices are essentially a surface phenomenon in the sense that they are derived from the \mathcal{FF} linked to the stellar models only via the effective temperature, surface gravity, and iron content [Fe/H], details of the stellar models caused by patterns of abundances enhanced in α -elements are of minor relevance. The point has been made clear by the systematic analysis of the issue made by Tantalò & Chiosi (2004). Therefore, the stellar models and companion SSPs by Girardi et al. (2000) and Girardi (2003, private communication) are fully adequate to the purposes of the present study.

The stellar models extend from the ZAMS up to either the start of the thermally pulsing AGB phase (TP-AGB) or carbon ignition. No details on the stellar models are given here; they can be found in Girardi et al.

(2000) and Girardi et al. (2002). Suffice it to mention that: (i) in low mass stars passing from the tip of red giant branch (T-RGB) to the HB or clump, mass-loss by stellar winds is included according to the Reimers (1975) rate with $\eta=0.45$; (ii) the whole TP-AGB phase is included in the isochrones with ages older than 0.1 Gyr according to the algorithm of Girardi & Bertelli (1998) and the mass-loss rate of Vassiliadis & Wood (1993); (iii) four chemical compositions are considered as listed in Table 1.

2.6 Library of stellar spectra

The library of stellar spectra is taken from Girardi et al. (2002). It covers a large range of the $\log T_{\text{eff}} - \log g -$ and $[M/H]$ space. No details are given here. Suffice to mention

- The basic spectra are from Kurucz ATLAS9 non-overshooting models (Castelli et al. 1997; Bessell et al. 1998) complemented with:
 - Blackbody spectra for $T_{\text{eff}} > 50,000$ K;
 - Fluks et al. (1994) empirical M-giant spectra, extended with synthetic ones in the IR and UV, and modified shortward of 4000\AA so as to produce reasonable $T_{\text{eff}}-(U-B)$ and $T_{\text{eff}}-(B-V)$ relations for cool giants;
 - Allard et al. (2000) DUSTY99 synthetic spectra for M, L and T dwarfs.

The theoretical broad-band colors used in this study are in the Johnson-Cousins-Glass UBVRIJHK system, using filter response curves from Bessell & Brett (1988) and Bessell (1990).

3 LINE ABSORPTION INDICES FOR SSPS

In this study we essentially adopt the large grids of line absorption indices recently calculated by Tantalò & Chiosi (2004) for SSPs over large ranges of chemical abundances, enhancement factors Γ , and ages. However we have slightly changed the ratio $[X_{el}/Fe]$ for some specific elements. More precisely, the abundance ratios for solar-scaled and α -enhanced mixtures with $\Gamma=0.35$ and $\Gamma=0.50$ are taken from Tantalò & Chiosi (2004) but for Ti for which lower $[Ti/Fe]$ are used. They are listed in Table 2, in which Columns (2), (3) and (6) show the abundance A_{el} of elements in logarithmic scale, columns (4) and (7) list the ratio $[X_{el}/Fe]$, and finally columns (5) and (8) show the ratio $[X_{el}/H]$ ¹.

First of all and in view of the discussion below it is worth reminding the reader the definition of three indices that are commonly used but which do not belong to the original Lick system. They are (Fe), [MgFe] and [MgFe]'

$$(\text{Fe}) = 0.5 \times (Fe5270 + Fe5335)$$

$$[\text{MgFe}] = \sqrt{\text{Mg}_b \times (0.5 \times Fe5270 + 0.5 \times Fe5335)}$$

¹ The complete grids of stellar tracks, isochrones, magnitudes, are available on the web site <http://pleiadi.pd.astro.it>, whereas SSPs colors, line absorption indices can be found on the web site <http://dipastro.pd.astro.it/galadriel>.

Table 2. Abundance ratios for the solar-scaled and α -enhanced mixtures adopted in this study. The abundances are the same as in Tantalo & Chiosi (2004) but for Ti for which lower $[\text{Ti}/\text{Fe}]$ ratios have been adopted: either $[\text{Ti}/\text{Fe}]=0$ (case a) or $[\text{Ti}/\text{Fe}]=0.20$ (case b). See the text for details).

Element	$\Gamma = 0$		$\Gamma = 0.35$		$\Gamma = 0.50$		Note	
	A_{el}	A_{el}	$[\frac{X_{el}}{F_c}]$	$[\frac{X_{el}}{H}]$	A_{el}	$[\frac{X_{el}}{F_c}]$		$[\frac{X_{el}}{H}]$
<i>O</i>	8.87	9.37	0.50	+0.1434	9.57	0.70	+0.2016	case a case b
<i>Ne</i>	8.08	8.37	0.29	-0.0666	8.49	0.41	-0.0936	
<i>Mg</i>	7.58	7.98	0.40	+0.0434	8.14	0.56	+0.0610	
<i>Si</i>	7.55	7.85	0.30	-0.0566	7.97	0.42	-0.0796	
<i>S</i>	7.21	7.54	0.33	-0.0266	7.67	0.46	-0.0374	
<i>Ca</i>	6.36	6.86	0.50	+0.1434	7.06	0.70	+0.2016	
<i>Ti</i>	5.02	5.65	0.00	-0.3566	5.89	0.00	-0.5013	
<i>Ti</i>	5.02	5.65	0.20	-0.1566	5.89	0.20	-0.2201	
<i>Ni</i>	6.25	6.27	0.02	-0.3366	6.28	0.03	-0.4731	
<i>C</i>	8.55	8.55	0.00	-0.3566	8.55	0.00	-0.5013	
<i>N</i>	7.97	7.97	0.00	-0.3566	7.97	0.00	-0.5013	
<i>Na</i>	6.33	6.33	0.00	-0.3566	6.33	0.00	-0.5013	
<i>Cr</i>	5.67	5.67	0.00	-0.3566	5.67	0.00	-0.5013	
<i>Fe</i>	7.50	7.50	0.00	-0.3566	7.50	0.00	-0.5013	

and

$$[\text{MgFe}]' = \sqrt{\text{Mg}_b \times (0.72 \times \text{Fe}5270 + 0.28 \times \text{Fe}5335)}$$

Going into a detailed description of the dependence of the line absorption indices for SSPs on age, chemical composition, Γ , is beyond the scope of this study. The reader is referred to Tantalo & Chiosi (2004) who have discussed these matters in great detail. Suffice it to show in Fig. 1 the temporal evolution of eight important indices, i.e. Mg_b , Mg_2 , H_β , $\langle \text{Fe} \rangle$, $[\text{MgFe}]$, $[\text{MgFe}]'$, NaD and C_24668 , for the following combinations of metallicity and Γ , namely $Z=0.008$ (solid lines) and $Z=0.070$ (broken lines), $\Gamma=0$ (heavy lines) and $\Gamma = 0.35$ (light lines). The age goes from 0.01 Gyr to 20 Gyr. It is worth noticing that the index Mg_2 does not depend on Γ .

Perhaps the most relevant result here is the variation of the indices with Γ . The easiest way of showing this is the H_β vs. $[\text{MgFe}]$ plane shown in Fig. 2, in which the range of values expected at varying metallicity (heavy solid lines), age (dotted lines), Γ and $[\text{Ti}/\text{Fe}]$ (hatched areas) as displayed. Each hatched area is enclosed between the two SSPs with the lowest and highest metallicity in our sample, i.e. $Z=0.008$ (left) and $Z=0.07$ (right) and two lines of constant age (14 Gyr bottom and 2 Gyr top). Along each SSP four values of the age are marked, so that other lines of constant age can be drawn. Let us consider the hatched areas corresponding to $\Gamma=0$, 0.35 and 0.5, independently of the value for $[\text{Ti}/\text{Fe}]$, either 0 or 0.2. These cases will be discussed separately below. At increasing Γ both H_β and $[\text{MgFe}]$ increase. While the effect on $[\text{MgFe}]$ is somehow expected, the one on H_β is more difficult to understand. The explanation is in the strong Response Functions for elements like N, O, Mg etc found by Tripicco & Bell (1995) and in the different way enhancing those elements affects the ratio F_i/F_c . In presence of enhancement, the spectrum over the three pass-bands defining the index H_β is more absorbed. However, absorption in the blue wing is larger than in the central band and in the red wing. Owing to this, the ratio F_i/F_c gets smaller so that H_β gets stronger. This trend is also confirmed by the new

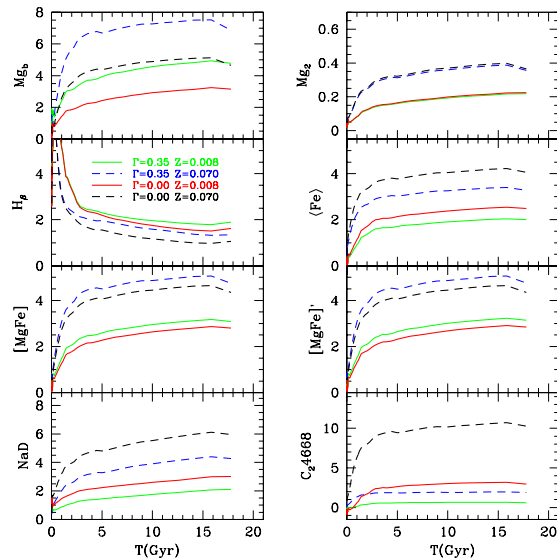


Figure 1. Evolution of eight indices (Mg_b , Mg_2 , H_β , $\langle \text{Fe} \rangle$, $[\text{MgFe}]$, $[\text{MgFe}]'$, NaD and C_24668) as function of the age. The heavy lines show the indices for solar-scaled partition of elements ($\Gamma=0$), whereas the thin lines show the same but for the partition of α -enhanced taken from Salasnich et al. (2000) ($\Gamma=0.3557$). Only two metallicities are displayed for the sake of clarity, i.e. $Z=0.008$ (solid lines) and $Z=0.07$ (dashed lines).

Response Functions calculated by Tantalo et al. (2004) using high resolution spectra (1\AA).

There is another important point to be addressed, which has already been touched upon by Tantalo & Chiosi (2004) and it is shown in Fig. 2 by the cases with the same Γ , either 0.35 or 0.5, and different $[\text{Ti}/\text{Fe}]$. In brief, at given metallicity Z , total enhancement factor Γ , and list of enhanced/depressed elements, the same Γ can be obtained by many patterns of $[X_{el}/F_c]$. For instance Tantalo & Chiosi (2004) have shown that at given Γ indices like H_β are very sensitive to the abundance ratio $[\text{Ti}/\text{Fe}]$. In their calculations several values of $[\text{Ti}/\text{Fe}]$ have been explored, i.e. $[\text{Ti}/\text{Fe}]=0$,

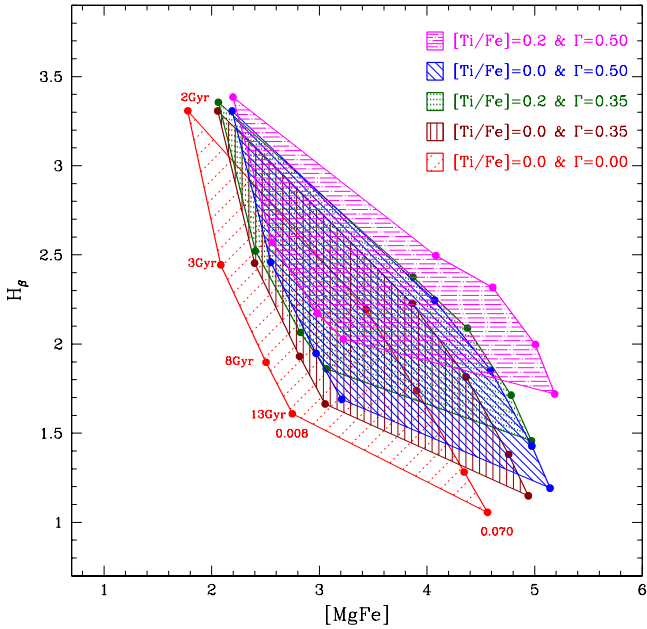


Figure 2. The H_β vs. $[MgFe]$ plane for different combinations of $\Gamma=0$, metallicity, and $[Ti/Fe]$ as indicated. Each hatched area is enclosed between the two SSPs with the lowest and highest metallicity in our sample, i.e. $Z=0.008$ (left) and $Z=0.07$ (right). Along each SSP four values of the age are marked so that the lines of constant age can be drawn. Four values of the age are, i.e. 2, 3, 8, and 14 Gyr. The different hatched areas correspond to different combinations of Γ and $[Ti/Fe]$ as indicated in the legend. Looking at this diagram one can easily single out the separate effect of the four parameters: age, metallicity, Γ and $[X_{el}/Fe]$ ($[Ti/Fe]$ in this case). See the text for more details.

0.20 and 0.63. The first choice implies that Ti is not considered as an α -element, the second one is based on the mean value measured by Gratton et al. (2003) for galactic metal-poor stars with accurate parallaxes, whereas the last choice comes from the old estimate by Ryan et al. (1991) for stars of the same type. In Fig. 2 we show the effect of varying $[Ti/Fe]$ from 0 to 0.2. Test calculations show that other elements like O, Mg, Ne, Ca etc. have a similar effect. The explanation is the same as before.

Since there is no unique pattern of abundance ratios as clearly shown by the above mentioned observational data, at given Z and Γ a sort of natural width for the indices has to be expected. The natural width we are talking about is provided by the difference $(I_{[X_{el}/Fe]} - I_{[X_{el}/Fe]})_{age, \Gamma, Z}$. It is soon evident that models with the same Z , Γ and age may have significantly different H_β and $[MgFe]$ (indices in general) depending of the detailed pattern of $[X_{el}/Fe]$ in use.

4 COMPOSING SSPS

Since the stellar content of a galaxy can be approximated by a manifold of SSPs of different age and metallicity, each of which weighed on the star formation rate, the indices of composite stellar populations can be derived in simple fashion without making use of sophisticated population synthe-

sis techniques requiring chemo-spectro-photometric models of galaxies (Tantalo et al. 1998).

Given the generic index $I_i^{SSP}(Y, Z, \Gamma, t)$, with the aid of eqn. (2) we derive the integrated fluxes of the SSP in the absorption feature and pseudo-continuum

$$\mathcal{F}_l(Y, Z, \Gamma, t) = \sum_i F_{l,i}^* N_i \quad (6)$$

and

$$\mathcal{F}_c(Y, Z, \Gamma, t) = \sum_i F_{c,i}^* N_i \quad (7)$$

Let us consider a composite object made of several SSPs with assigned composition, total enhancement and age – $(Y_j, Z_j, \Gamma_j, t_j)$ – each of which intervening in suitable percentages β_j . This parameter measures the intensity of star formation assigned to each component, in other words it is the fraction of the galaxy mass engaged in each SSP. The integrated fluxes are

$$\mathcal{F}_l^{comp} = \sum_j \beta_j \mathcal{F}_{l,j}(Y_j, Z_j, \Gamma_j, t_j) \quad (8)$$

and

$$\mathcal{F}_c^{comp} = \sum_j \beta_j \mathcal{F}_{c,j}(Y_j, Z_j, \Gamma_j, t_j) \quad (9)$$

The total mass is the sum of the SSP mass over all the components and re-normalization of the fluxes can be applied if required. The composite indices are then derived by inserting the above integrated fluxes into eqn. (2).

For the sake of illustration we consider the case of an old galaxy, represented by a SSP with solar composition and no enhancement of α -elements ($Z=0.019$ and $\Gamma=0$), which at the age of 10 Gyr suffers a burst of stellar activity represented by another SSP of the same Z and Γ . The old galaxy is labelled by $j=1$ and the burst component by $j=2$. Three cases of the burst intensity are examined, i.e. $\beta_1=0.98$ and $\beta_2=0.02$, $\beta_1=0.90$ and $\beta_2=0.10$, $\beta_1=0.80$ and $\beta_2=0.20$. Once the burst has occurred the photometric properties of the composite object are described with the age step of the young SSP in order not to loose in the time resolution of magnitudes, colors, and indices. In simulations of this type, both the old and the young component are let evolve with time from the burst epoch to the present. The results are shown in the panels of Fig. 3 and Fig. 4. The left panel of Fig. 3 is the color (B–V) vs. age (in Gyr); whereas the right panel is the H_β vs. age. The left panel of Fig. 4 is the plane (U–B) vs. (B–V), whereas the right panel is the H_β vs. $[MgFe]$ plane. For the sake of clarity, the burst is displayed only for ages older than 0.1 Gyr because its path in the two colors and/or two indices planes for younger ages is quite complicated and difficult to describe in a simple fashion. In the left and right panels of Fig. 3 the age structure of the bursting mode is clear. The color (B–V) and index H_β are suddenly rejuvenated at the onset of the burst: (i) (B–V) may get very blue, the peak value depends on β_2 , and then fade down toward the typical color of an old object as the age increase from 10 Gyr up to 16 Gyr. The same for H_β .

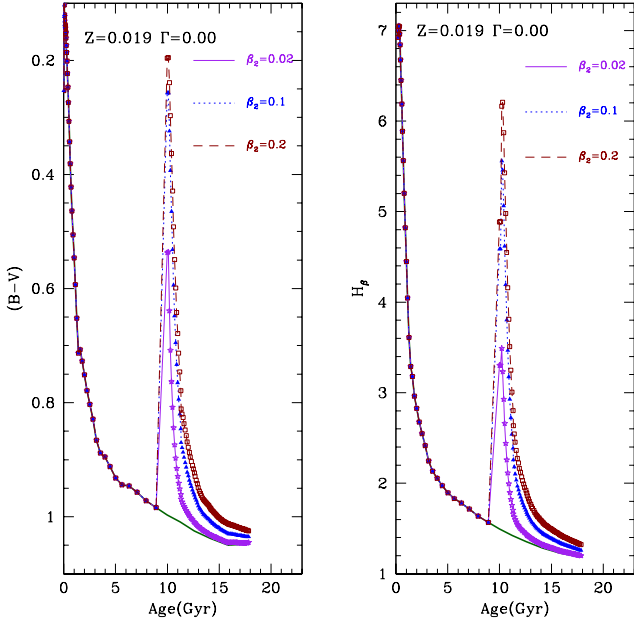


Figure 3. A burst of star formation of different intensity (as indicated) is let occur in an ideal galaxy represented by a SSP with $Z=0.019$ and $\Gamma=0$ at the age of 10 Gyr. The composite object is then followed up to the age of 16 Gyr. **Left Panel:** $(B-V)$ vs. age. **Right Panel:** H_β vs. age.

(ii) In all simulations both H_β and $(B-V)$ keep memory of the bursting activity for long time. Both indeed tend to be lower and higher, respectively, than the pure passive evolution indicated by the solid heavy line. In the planes $(U-B)$ vs. $(B-V)$ and H_β vs. $[MgFe]$ of Fig. 4, the composite object performs wide loops, the extension and width of which are functions of the intensity β_2 . The complete path of the bursting object is better shown in Fig. 5 below.

Another interesting plane to look at is the superposition of two SSPs, one old and the other young (in different percentages as above, but in which the age of the old SSP is kept fixed whereas that of the young one is let vary from 0.01 Gyr to the age of the old component in suitable steps. These simulations allow us to span the whole range of possible combinations of ages for the two SSPs and the whole range of values in any two-indices plane at varying intensity and age of the burst. In other words, any point in these plane is a picture of the composite galaxy taken at a certain age of the burst. Simulations of this type are shown in Fig. 5 for the typical age of the old SSP of 13 Gyr. The apparently strange behavior of the SSP path at increasing age of the burst deserves some explanation. The bell-shaped trend of H_β has already been explained by Buzzoni et al. (1994). In brief for strong H_β absorption (as in young SSPs and/or burst of star formation), the Stark wings of the feature overflow the Lick wavelength window, and enter the side bands depressing the pseudo-continuum. As a result, the H_β index peaks when the SSP is dominated by B5-A0 stars and fades for earlier and later spectral types. This is mirrored in the path of the composite SSP with the contribution from each component weighed on its percentage. It is worth noticing

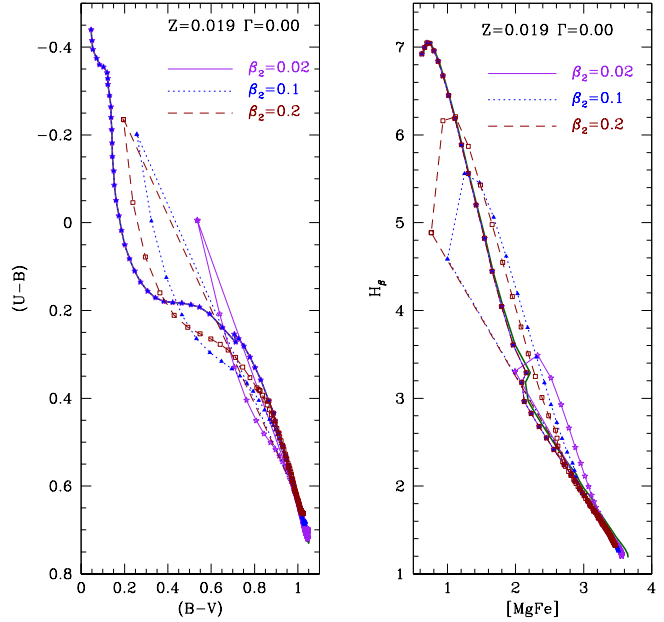


Figure 4. The same as in Fig. 3. **Left panel:** the $(U-B)$ vs. $(B-V)$ plane. **Right Panel:** the H_β vs. $[MgFe]$ plane.

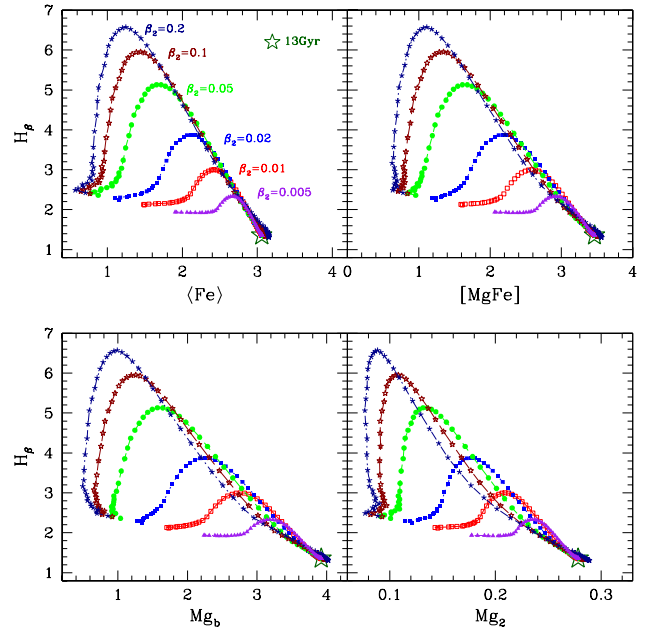


Figure 5. Composite SSPs: young SSPs of any age and metallicity $Z=0.040$ are superposed to an old SSP with the age of 13 Gyr and the metallicity $Z=0.019$. The age of the old SSP is kept constant. Different percentages (β_2) for the young component are considered as indicated. The percentage of the old component is $\beta_1=1-\beta_2$. The various panels show four different diagnostic planes.

that a galaxy caught at the very early stages of its bursting activity would appear as an object with unusually low indices. We will come back to this later on.

5 INDEX-INDEX DIAGNOSTICS: AGE OR CHEMISTRY?

The sample of galaxies we intend to analyze is derived from two sources of data, namely the “*IDS Pristine*” catalog by Trager (1997) for the central regions of normal galaxies – it contains also the González (1993) list –, and the catalog by Longhetti et al. (2000) for pair- and shell-galaxies (i.e. only objects with clear signs of interaction). The latter sample is given in Table 3². The H_β vs. [MgFe] plane for all the galaxies in question is shown in the left panels of both Figs. 6 and Fig. 7 to facilitate the comparison with the theoretical simulations we are going to present. It is worth calling attention on the striking similarity between normal and interacting galaxies, and the very smooth but steeper slope of the data as compared to that of SSPs of given metallicity (see Fig. 2). In the following we will refer to it as the *nearly vertical distribution* along the H_β axis.

5.1 A toy galaxy model

Bressan et al. (1996) and Longhetti et al. (2000) suggested that the distribution of galaxies in the H_β vs. [MgFe] plane may reflect secondary episodes of star formation superposed to an old stellar component. In the following, we intend to explore further this idea by means of MonteCarlo simulations based on the Longhetti et al. (2000) toy model of galaxy evolution.

The complex star formation history of an early-type galaxy is reduced to a burst of relatively recent star formation superposed to the bulk population made of old stars. These latter are in turn represented by a SSP whose age is randomly selected between the ages T_1 and T_2 . The young stellar component, formed during the recent burst of star formation, is represented by a SSP whose age is randomly selected between T_2 and a lower limit T_3 . Typical values for the age limits are: $T_1=13$, $T_2=10$, and $T_3=0.1$ Gyr. The time-scale of the two star formation event are always assumed to be short compared to all other relevant timescales (ages, and Hubble time).

Since we are interested in guessing the minimum threshold above which the secondary episode gets importance in affecting the line strength indices, we will consider only the case in which the secondary episode involves a minor fraction of the galaxy mass. Typical values for the strength of the primary and secondary burst β_1 and β_2 , respectively, measuring the percentage of the total galaxy mass turned into stars, are $\beta_1=0.98$ and $\beta_2=0.02$.

The metallicity Z_1 of the old stellar component is randomly selected between 0.008 (50% of the solar value) and 0.07 (3.25 the solar value). We have also built a set of simulations in which the metallicity of the old component is

forced to linearly increase from 0.008 and 0.07 over the age range T_1 to T_2 . The metallicity Z_2 of the young component is randomly chosen over the whole range (i.e. from $Z=0.008$ to $Z=0.07$), thus simulating the widest range of possibilities, going from acquisition of external less processed gas to chemical enrichment during the burst.

The simulations are first performed for solar partitions of elements, i.e. $\Gamma=0$ and then for $\Gamma \neq 0$ (another dimension is added to the problem).

Finally, random errors are applied to the model indices to better simulate the observations. Using the data by Trager (1997) we calculate the mean relative errors $\langle \Delta I / I \rangle_0$ as reported in Table 4. The error affecting an index is randomly evaluated according to

$$\Delta I = - \left\langle \frac{\Delta I}{I} \right\rangle_0 I + 2 \times \epsilon \left\langle \frac{\Delta I}{I} \right\rangle_0 I \quad (10)$$

where ϵ is a random number between 0 and 1.

5.2 Large scatter in age and metallicity of the bulk population

This is the simplest interpretation of the distribution of the galaxies in the H_β vs. [MgFe] plane. Neglecting important effects due to enhancement in α -elements and recent stellar activity, matching the observational range of the data would require the bulk population of early type galaxies being formed in different epochs from galaxy to galaxy over a time-scale comparable to the Hubble time. In the central panel of Fig. 6 we show a simulated sample of 100 objects for which the following parameters are assumed: $T_1=13$ Gyr, $T_2=2$ Gyr, $\beta_1=1$, no increase of the metallicity in this time interval, no later bursts of stellar activity, and finally $\Gamma=0$. The models galaxies distribute along the SSP lines of different metallicity according to their age. The simulation significantly differs from the observational data shown in left panel of Fig. 6. Even if this view could be fitted into the classical hierarchical scheme of galaxy formation, it can be hardly sustained because it would predict spectrophotometric properties not fully compatible with the observational data for EGs.

5.3 Random bursts of star formation

Bursts of star formation (from one to several) superposed to an old dominant population of stars seem to be more plausible and yield better results. Galaxies are conceived as old, nearly coeval systems, their population being approximated by a single SSP with age between 10 and 13 Gyr; this age range agrees with the current age estimate of EGs in rich clusters (Bower et al. 1998). A burst of stellar activity is added at an age randomly chosen in the interval T_2-T_3 . Two different prescriptions for the metallicity are adopted as described in Section 5.1 above. Finally all the simulations are for $\Gamma=0$. The maximum intensity of the superposed burst amounts to 2% of the total mass, i.e. $\beta_1=0.98$ and $\beta_2=0.02$.

The simulations of this type are made at increasing complexity. Since they essentially confirm what already found by Longhetti et al. (2000) we limit ourselves to discuss the results and to highlight the point of disagreement

² We remind the reader that the values of [MgFe] listed in Table 4 of Longhetti et al. (2000) have been calculated using the wrong expression $[\text{MgFe}] = \sqrt{\text{Mg}_b \times \text{Fe}5270 + \text{Fe}5335/2}$

with the observational data without showing any simulation in detail:

(i) Stronger bursts of star formation (i.e. engaging more than 2% of the mass) are not suited as they would predict too high values of H_β and too many *young* objects.

(ii) The expected distribution of objects with respect to the H_β index is at variance with the observational one. Indeed models of this type predict a bimodal distribution, whereby the old galaxies (those for which the burst is almost as old as the bulk of their stellar populations) clump together in the lower portion of the diagram, whereas the “young” objects (those with very young bursts) form a tail extending to high values of H_β .

(iii) Nevertheless, the burst alone cannot explain the smooth distribution observed at low H_β values. This is because the H_β index of a stellar population for which the 2% of the mass is composed by “young” stars and the remaining 98% by an old component, reaches the observed high values, but, fading very rapidly with the age of the “young” component, has low probability to match the intermediate observed values. Slowing down the index decrease (corresponding to the aging of the “young” component) by increasing the percentage of mass involved by the young burst produces a uncomfortably large fraction of objects in the upper part of the diagram. A complex interplay between burst intensity and mean age of the stellar population should then take place, with the old bursts being on average stronger than the recent ones. It must be said, however, that when the burst itself is larger than a few percent of the total mass, the definition of the average age of the bulk of the stellar population becomes a problem.

(iv) The difficulty is partially cured assuming that the *old* population has an average age spreading over a significant fraction of the Hubble time (say down to $T_2 \simeq 5$ Gyr). This is meant to indicate that either the object has been growing for such a long time with a low star formation rate, or that its major star formation activity was not confined to an early epoch. The young component is left to occur. It appears immediately that the observed smooth distribution in the H_β index together with the young tail can be much better reproduced with such a kind of models, see Longhetti et al. (2000) for details.

(v) Another problem arises if the metallicity is randomly selected. The distribution of the model galaxies in the left panel of Fig. 6 strictly follows the path of a SSP, whereas the data run much steeper. We take this point to invoke the existence of a relation between the age of the bulk stellar population and its average metallicity and to apply the ULME. The simulations better fit the data.

The right panel of Fig. 6 shows our final experiment incorporating all the hints we have been discussing so far. The simulations are based on the following parameters and assumptions: $T_1=13$ Gyr, $T_2=5$ Gyr, $T_3=0.1$ Gyr, $\beta_1=0.98$, $\beta_2=0.02$, average metallicity of the bulk of the stellar population forced to linearly increase from $Z=0.008$ to $Z=0.070$ over the time interval T_1 to T_2 . Thanks to the combined effect of the large age and metallicity spread for the bulk population, the distribution in H_β vs. $[\text{MgFe}]$ plane is *nearly vertical*. The larger range of metallicity is necessary to maintain a significant dispersion in $[\text{MgFe}]$, because age differences tend to compensate metallicity differences. If the latter interpretation is correct, it suggests that young early-type

galaxies in the field are on average more metal-rich than old systems, with an average metallicity gradient of about $\Delta \log(Z)/\Delta \log(t) \simeq -0.7$, the latter value being very dependent on the younger limit of the bulk age.

The main conclusion out of these simulations is that in addition to the mass dominating old population, which however has to be built up over a large time interval and under a suitable age-metallicity relationship, sprinkles of stellar activity in the recent or very recent past ought to be considered in nearly all galaxies to reconcile theory and observations. *However, that all galaxies have to go through recent star forming activity is perhaps too demanding and other alternatives should be explored.*

5.4 The α -enhancement alternative

The results obtained by Tantalo & Chiosi (2004) for SSPs of the same age and metallicity but different degrees of enhancement in α -elements offer a third plausible explanation. The bottom line of the model is best explained by comparing the theoretical models in the H_β vs. $[\text{MgFe}]$ plane of Fig. 6 (central and right panels), with the observational data (left panel). Several points are soon evident:

(i) The majority of galaxies (those with $H_\beta \leq 2$) are fully compatible with being very old objects of the same age (say about 13 Gyr) but a different degree of enhancement in α -elements going from $\Gamma=0$ to $\Gamma=0.5$ (taking the so-called natural width caused by a possible variation in single elemental species into account). As a matter of fact, an old galaxy (say a 10-13 Gyr object) being shifted to higher H_β by high Γ and/or $[X_{el}/\text{Fe}]$ ($[\text{Ti}/\text{Fe}]$ as a prototype) could lie in the same region occupied by a galaxy of significantly younger age and solar abundance ratios. At least part of the scatter along the H_β axis could be due to a different degree of enhancement in α -elements.

(ii) Only for galaxies with $H_\beta > 2$, unless their enhancement factor Γ and abundance ratios $[X_{el}/\text{Fe}]$ (like $[\text{Ti}/\text{Fe}]$) are larger than the above limits, the presence of secondary star forming activity ought to be invoked.

(iii) Looking at the position of models of constant metallicity and age but different Γ and/or $[X_{el}/\text{Fe}]$ (for instance $[\text{Ti}/\text{Fe}]$), they scatter along a *nearly vertical* line. This implies that the metallicity relationship invoked for the bulk old population is no longer required. The *vertical* distribution of the data is simply caused by the compensatory effect of different combinations of Z , Γ and $[X_{el}/\text{Fe}]$ ($[\text{Ti}/\text{Fe}]$ in our case).

(iv) Secondary episodes of star formation are no longer a common feature to all galaxies, but an exceptional event limited to a small number of them. This agrees with the age distribution obtained by Tantalo & Chiosi (2004).

The α -Model is confirmed by the MonteCarlo simulations shown in the left and right panels of Fig. 7. In the left panel we show the case of old galaxies with no secondary activity: the bulk population spans the age range given by $T_1=13$ Gyr and $T_2=10$ Gyr with $\beta_1=1$, whereas the metallicity and α -enhancement span the whole range for the parameters Z , Γ , and $[X_{el}/\text{Fe}]$ ($[\text{Ti}/\text{Fe}]$ taken as a measure of the natural width). Since there is no further star formation activity $T_3=10$ Gyr and $\beta_2=0$. The models essentially match the bulk of data, i.e. galaxies with $H_\beta \leq 2$, and yield a distribution in the H_β vs. $[\text{MgFe}]$ plane which is *nearly vertical* (no

Table 4. Relative errors for the theoretical simulations.

$\langle \Delta H_\beta / H_\beta \rangle$	$\langle \Delta \text{Mg}_b / \text{Mg}_b \rangle$	$\langle \Delta \text{Mg}_2 / \text{Mg}_2 \rangle$	$\langle \Delta C_{24668} / C_{24668} \rangle$	$\langle \Delta \text{NaD} / \text{NaD} \rangle$	$\langle \Delta \langle \text{Fe} \rangle / \langle \text{Fe} \rangle \rangle$	$\langle \Delta [\text{MgFe}] / [\text{MgFe}] \rangle$
0.136	0.059	0.026	0.009	0.054	0.073	0.047

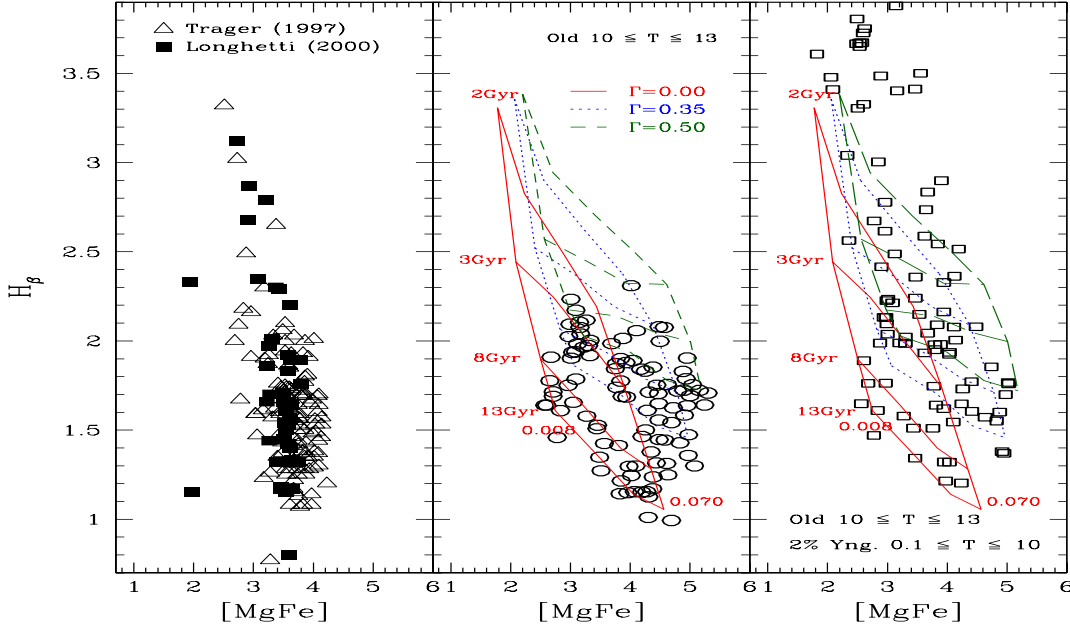


Figure 7. Observational data and MonteCarlo simulations for the α -Model. **Left Panel:** The normal galaxies by Trager (1997) indicated by the open triangles and the shell- and pair-galaxies of Longhetti et al. (2000) indicated by the filled squares. **Central Panel:** old galaxies formed in the time interval $T_1=13$ to $T_2=10$ Gyr and no later star formation activity ($\beta_1=1$ and $\beta_2=0$). Each model galaxy has a metallicity and enhancement factor Γ randomly chosen from the whole range, i.e. $0.008 \leq Z \leq 0.07$ and $0 \leq \Gamma \leq 0.35$. No universal enrichment law is considered. Thanks only to the different combinations of Z and Γ (different chemical compositions in general), the model galaxies span a large range of the observational values for H_β and $[\text{MgFe}]$. **Right panel:** the same as before, but now a small percentage of a young population has been added, i.e. $\beta_1=0.98$ and $\beta_2=0.02$, whose age randomly varies in the interval $0.1 \leq T_3 \leq 10$ Gyr. The secondary burst of star formation has been included to get full coverage of the observational H_β range in particular for those galaxies with $H_\beta > 2.5$. In both panels the meaning of the various lines (solid, dashed and dotted) is the same as in Fig. 2.

memory of the SSPs path). In the right panel we show the same but allowing for recent burst to occur, i.e. $T_3=0.1$ Gyr. The burst intensity is for $\beta_2=0.02$. But for the few galaxies clearly caught in the burst mode (those with $H_\beta > 2$), the two theoretical distributions are nearly identical and both fairly well reproduce the observational data.

These simulations open the gate to an interesting alternative explanation, i.e. that the large scatter in H_β and $[\text{MgFe}]$ is predominately caused by a spread in the chemical parameters metallicity Z and enhancement factor Γ rather than metallicity and age in the bulk population of a galaxy. Secondary activity of star formation is unavoidable only for a minority of objects.

The scatter in Z , Γ and also individual $[X_{el}/Fe]$ of the dominant old stellar component could be attributed to different kinds of star formation at the very early epochs, perhaps related to the physical conditions in the proto-galaxy affecting not only the intensity and duration of the star formation process, but also the initial mass function of the stars and the abundance ratios in turn. We will touch upon this point later.

6 DISCUSSION

Testing the α -Model. To corroborate the suggestion that the scatter in the H_β vs. $[\text{MgFe}]$ plane for most galaxies is due the chemical parameters Γ , Z , and perhaps $[\text{Ti}/\text{Fe}]$ we perform here a few *ad hoc* experiments.

First of all, we test a model with a very narrow age range for the old component and no subsequent star formation. The test is meant to isolate the sole effect of the chemical abundances. The model is characterized by the parameters: $T_1=13$ Gyr, $T_2=12$ Gyr, $\beta_1=1$, $T_3=12$ Gyr, and $\beta_2=0$. While no ULME is considered, the metallicities, Γ s and $[X_{el}/Fe]$ s (at present $[\text{Ti}/\text{Fe}]$) are let span the whole range. The simulations are shown in left panel of Fig. 8 correlating Mg_b with $[\text{MgFe}]$. The choice of these two indices is based on the notion that $[\text{MgFe}]$ is nearly independent on Γ , whereas Mg_b does. Both are sensitive to the age and metallicity even if some degree of degeneracy is present. On purposes we avoided H_β because of its equal sensitivity to all the parameters in question. In this plane we also displays the theoretical areas corresponding to the different combinations of Γ and $[\text{Ti}/\text{Fe}]$, metallicities, and ages. Each area is bounded by

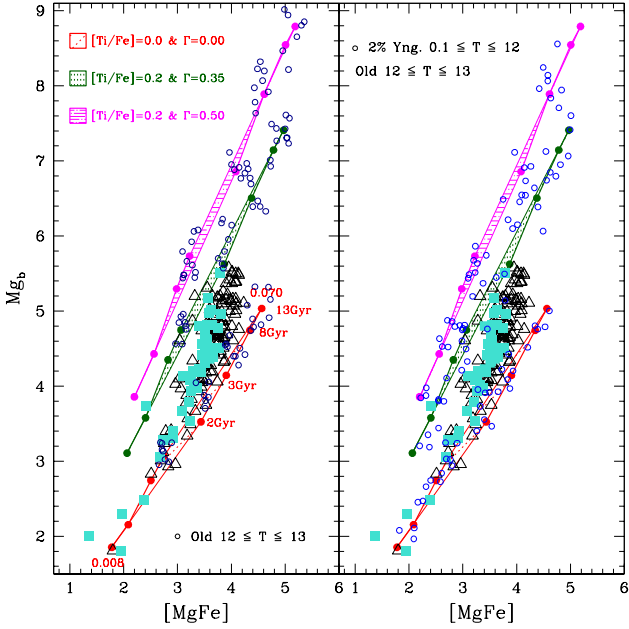


Figure 8. MonteCarlo simulations of the type shown in Fig. 7 but with a narrower age range for the old component. They are aimed to better constrain the metallicity and enhancement factor suited to the data. **Left Panel:** models with only the very old component. **Right Panel:** models with both old and young stellar populations. In both panels the simulations are indicated by open circles and all other symbols have the same meaning as in Figs. 2 and 7. In this plane real galaxies seem to fall in the ranges $0 \leq \Gamma \leq 0.3$ and $0.008 \leq Z \leq 0.05$.

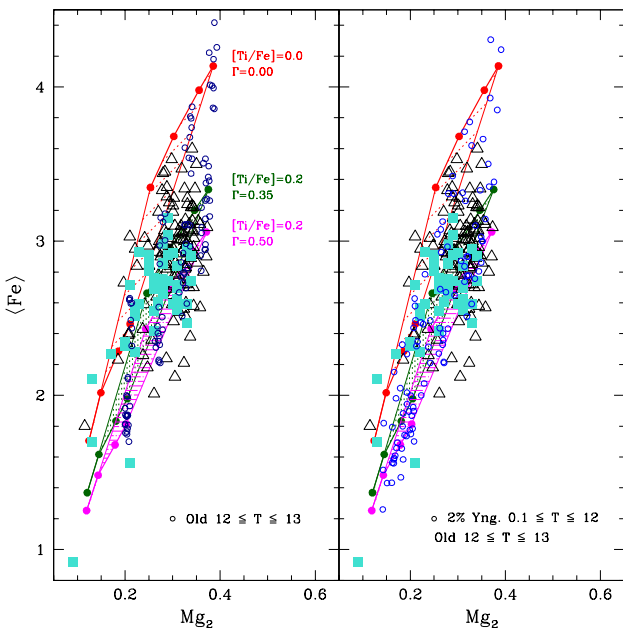


Figure 9. The same as in Fig. 8 but for the $\langle \text{Fe} \rangle$ vs. Mg_2 plane. Now the data seem to be compatible with $0.35 \leq \Gamma \leq 0.50$ and metallicities extending up to $Z=0.07$.

the SSPs with the lowest ($Z=0.008$) and highest ($Z=0.070$) metallicities, the two heavy lines along which four values of the age are marked (2, 3, 8, and 13 Gyr). It is worth noticing the good resolving power of Mg_b only for Γ and large insensitivity to all remaining parameters. Different values of $[X_{el}/\text{Fe}]$ ($[\text{Ti}/\text{Fe}]$ in this case) have in practice no effect. Furthermore, the age and metallicity are nearly degenerate. The open circles are the simulations, the filled squares are the data by Longhetti et al. (2000), and finally the open triangles are those by Trager (1997). Secondly, we re-examine in the same plane the simulations shown in Fig. 7, in which a wider age range for the old component is adopted. All remaining ingredients are the same as above. These model are shown in the right panel of Fig. 8. Comparing data with theory, we would conclude that in both cases Γ in the range 0 to 0.35 and $Z \leq 0.07$, likely 0.05, are best suited, the only difference between the two type of models is that in presence of a burst the left-lower corner of the panels is populated (i.e. $\text{Mg}_b \leq 2$ and $[\text{MgFe}] \leq 3$). In any case the large dispersion of the bulk population in the H_β vs. $[\text{MgFe}]$ plane is once more compatible with all galaxies being old and spanning a large range of Γ s and Z s. The large age dispersion (say from 13 to 5 Gyr) and the occurrence of a later burst of activity are no longer unavoidable results and/or hypotheses. Only a few galaxies seem to require a later burst of star formation.

However, the upper limits suggested by the Mg_b vs. $[\text{MgFe}]$ plane are not firmly established as different conclusions would be derived by looking at another diagnostic plane such as $\langle \text{Fe} \rangle$ vs. Mg_2 shown in Fig. 9. All the symbols have the same meaning as in Fig. 8. From this diagram one would indeed conclude that Γ falls in the range 0.35 to 0.5, that high metallicities (up to $Z=0.07$) are likely to occur, and finally that galaxies with $\Gamma=0$ and metallicities larger than solar or so are not there. Since Mg_2 seems not to depend on Γ and $\langle \text{Fe} \rangle$ is likely more sensitive to both Γ and Z than other indices, we would favor the hints arising from this diagnostic plane with respect to the previous ones.

Two Template Galaxies. It may be worth of interest here to closely inspect some of the galaxies in the samples paying major attention to those with unusually high H_β and/or very low $[\text{MgFe}]$. To this aim three sources have been used: Trager (1997); Longhetti et al. (2000) for the indices and central velocity dispersions, Burstein et al. (1997) for colors, masses, luminosities. The data are listed in Table 5. We have not considered RR24a and RR24b because of their negative H_β .

Without going into a detailed discussion of all these objects, we may still make several points:

(i) Adopting $(B-V)=1.00 \pm 0.05$ as the typical mean value for early-type galaxies (Burstein et al. 1997), those with strong H_β tend to be bluer than normal galaxies by $\Delta(B-V)=0.05$ to 0.10 up to the extreme case of NGC 3156 with 0.28. Furthermore there seems to be a correlation between $(B-V)$ and H_β : $(B-V)$ gets redder at decreasing H_β .

(ii) Looking at the time dependence of $(B-V)$ (other blue colors have the same behavior) shown in Fig. 4 owing to the very fast decline past the occurrence of the burst, colors in the range 0.8 to 0.9 are recovered after 1.5 Gyr or so (the exact value depends on the intensity of the burst), which is the age of the young component

(iii) From the position of a galaxy suspected to be in the burst or post burst activity because of its unusual in-

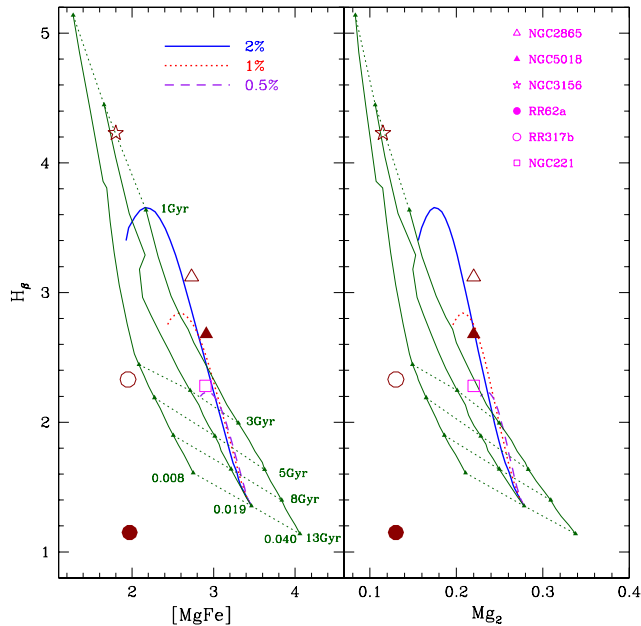


Figure 10. Age estimate of the last episode of star formation in a few galaxies with unusual values of H_β and/or $[MgFe]$ (Left panel) and Mg_2 (Right Panel). The galaxies indicated with different symbols are listed in the Right Panel. In each panel we plot three SSPs with different metallicity, $Z=0.008$, 0.019 , and 0.040 as indicated, along which five values of the age are marked, i.e. 13, 8, 5, 3 and 1 Gyr, and the corresponding lines of constant age are drawn (thin dotted lines). Finally, we show the locus expected for composite galaxies, in which to a population with the age of 13 Gyr and metallicity $Z=0.019$, an burst of arbitrary age and different intensity is added. The metallicity of the young component is however the same as the old one ($Z=0.019$). The intensities are $\beta_2=0.005$ (long dashed line), 0.01 (heavy dotted line), and 0.02 (solid line). Along each curve the age increases from the minimum plotted value 0.1 Gyr to 13 Gyr. The position of M32 is compatible with various combinations of T_B and β , for instance $T_B \simeq 1$ Gyr and $\beta_2=0.005$ or $T_B \simeq 2-3$ Gyr and β_2 in the range 0.01 to 0.02. At given β_2 , the burst age will increase if higher metallicities for the young component are considered.

indices in planes for composite systems like those presented in Fig. 5 on one hand we may get another estimate of the burst age, on the other hand we may check the consistency of the whole picture. For the sake of illustration, we discuss here the case of NGC 5018, a giant elliptical galaxy with total mass $M=1.24 \times 10^{11} M_\odot$, luminosity $L_B = 5.43 \times 10^{10} L_\odot$, central velocity dispersion $\Sigma_0=223$ km/s, $H_\beta=2.30$, and $Mg_2=0.211$. Long ago, Bertola et al. (1993) have classified NGC 5018 as a giant, chemically unevolved galaxy consisting of M32-like stars, and Leonardi & Worthey (2000) have suggested that the central regions of NGC 5018 are dominated by an intermediate-age population. Along the same vein, is the very recent study by Buson et al. (2004, private communication) who have stressed the close similarity between M32 (NGC 221) and NGC 5018. The similarity concerns the indices as shown by the entries of Table 5, the (B-V) colors, and the spectrum from 2000\AA to 4700\AA (Buson et al. 2004). They have also made the point that since M32 (at least in the central regions) is commonly considered to be dominated

by a population whose age is about 3 Gyr (Freedman 1989, 1992; Trager et al. 2000b,a; Longhetti et al. 2000) the same should occur for NGC 5018. However, the reality may be more articulated than this simple scheme. Studies of the stellar content and other properties of M32 have pointed out that the bulk population could be as old as that of globular clusters, e.g. see the discussion by Bressan et al. (1994) and references therein, and by Grillmair et al. (1996). Bressan et al. (1994, 1996) have argued that the young stellar component in M32 could result from a recent burst of activity superposed to the pre-existing, old stellar content. Is NGC 5018 experiencing the same? To check this possibility, in Fig. 10 we plot M32, NGC 5018 and other galaxies of Table 5 on to the H_β vs. $[MgFe]$ and Mg_2 planes and compare them with single SSPs of different age and metallicities and composite SSPs in which bursts of different intensity and age are superposed to an old dominant component. In the first case we recover the standard solution, i.e. M32 is an object whose stellar content is about 3-4 Gyr, whereas in the second case M32 is an old object (say 10-13 Gyr) on the top of which a young component (1-2% of the total mass) is present. The age of this is about 1 Gyr. An old galaxy, which underwent a burst of activity say 1 Gyr ago, would appear as a brand newly formed galaxy with the age of about 3-4 Gyr. The same analysis can be extended to other galaxies of Table 5. A special remark is due to the three galaxies with very low $[MgFe]$: we exclude RR317b because it shows evidence of emission $[OII](3712\text{\AA})$ as already pointed out by Longhetti et al. (2000). The case of NGC 3156 is trivial because of its strong H_β : it is indeed fully compatible with theory if undergoing a burst of star formation. We are left with RR62a for which not very much can be said: it follows the same μ_e-R_e relationship of ordinary galaxies, but it deviates from the Hamabe-Kormendy relationship (Hamabe & Kormendy 1987). It could be a old, low metallicity galaxy which according to Gorgas et al. (1993) should fall into the bottom left corner of the H_β vs. $[MgFe]$ plane. Alternatively it could be old galaxy which is just starting (or undergoing) a burst of star formation as indicated by the results for composite SSPs shown in Fig. 5.

The Coma EGs. We have already mentioned that EGs in Coma (Jørgensen 1999) have systematically higher values of H_β than the local galaxies. The minimum values is $H_\beta=1.5$. Repeating the same analysis we have made for the Trager (1997) and Longhetti et al. (2000) samples we would come up with the conclusions: (i) The α -Model may hold good even in this case. (ii) The Coma galaxies have a higher degree of enhancement than the local ones. A rough estimate is $\Gamma \geq 0.3$. Supporting this idea is the estimate for the age of Coma's EGs by Poggianti et al. (2001) who find a mean age older than about 9 Gyr; the estimate of the ratio $[Mg/Fe]$ by Jørgensen (1997); Jørgensen (1999) who finds $[Mg/Fe]=0.3$ to 0.4 as the central velocity dispersion $\log \Sigma_0$ increases of 0.4 dex; and finally the recent study by Mehlert et al. (2003) who find $[\alpha/Fe]$ ratios in the range 0.15 to 0.4. The mean degree of enhancement in EGs of the Coma Cluster seems to be at least 0.1 dex higher than in the local field galaxies. **α -Enhancement in EGs: Data and Theory.** The occurrence of the α -enhancement in early-type galaxies is currently attributed to the duration of the star forming period and the different contribution to chemical enrichment by Type Ia and Type II supernovae (see Matteucci 1997, for

Table 5. Selected galaxies: seven indices on the Lick system; M is the mass in solar units inside the effective radius; L_B is the B-luminosity in solar units; Σ_0 is the central velocity dispersion in km/s.

Name	H_β	Mg_2	Mg_b	Fe52	Fe53	(Fe)	[MgFe]	(B-V)	logM	L_B	Σ_0
Galaxies with $H_\beta \geq 2.5 \pm 0.2$											
NGC2865	3.12	0.220	3.28	2.34	2.22	2.28	2.73	0.83	10.517	10.241	208
NGC5018	2.68	0.220	3.31	2.89	2.24	2.56	2.91	0.85	11.094	10.736	247
E2400100b	2.79	0.210	3.79	3.12	2.33	2.71	3.21	0.82			223
RR101b	2.35	0.230	3.67	2.83	2.35	2.64	3.08	0.88			210
RR187b	2.80	0.220	3.40	2.69	2.34	2.51	2.92	0.93			144
NGC2863	3.02	0.208	3.12	2.65	2.20	2.43	2.88				87
NGC4742	3.32	0.185	2.83	2.50	1.97	2.23	2.51				105
NGC5061	2.65	0.275	3.93	2.97	2.83	2.90	3.38	0.86	10.925	10.586	191
Galaxies with $2 \pm 0.2 \leq H_\beta \leq 2.5$											
RR297a	1.97	0.270	4.08	2.89	2.32	2.60	3.26				177
RR387a	2.20	0.290	4.48	3.08	2.74	2.91	3.61				187
RR405b	1.89	0.340	4.81	2.72	2.76	2.74	3.63				207
RR409a	1.89	0.290	4.51	3.02	3.28	3.15	3.77				187
NGC221	2.18	0.197	2.93	2.94	2.53	2.73	2.83	0.84	8.592	8.074	77
NGC636	1.94	0.286	4.08	3.30	2.80	3.05	3.53				162
NGC1283	1.93	0.288	4.66	3.07	2.58	2.82	3.63	0.92	11.327	10.454	236
NGC1374	1.81	0.325	5.37	3.06	2.59	2.83	3.90	0.94	10.782	9.929	187
NGC1521	2.00	0.284	4.32	3.79	3.11	3.45	3.86	0.95	11.378	10.677	223
NGC1573	1.85	0.344	5.02	2.63	2.52	2.58	3.60				272
NGC1700	2.00	0.278	3.75	3.48	3.19	3.33	3.53	0.92	11.141	10.795	226
NGC2636	1.90	0.225	3.57	2.87	2.82	2.84	3.19				85
NGC2888	2.49	0.237	3.41	2.65	2.20	2.43	2.88				87
NGC3605	2.03	0.241	3.67	3.14	2.89	3.02	3.33	0.87	10.062	9.205	103
NGC3610	1.92	0.270	3.83	2.91	2.65	2.78	3.26				159
NGC3640	1.87	0.272	3.49	2.92	3.08	3.00	3.24	0.93	10.801	10.249	176
NGC3873	1.75	0.292	4.66	2.99	3.09	3.04	3.76				243
NGC4033	1.86	0.266	4.38	3.13	2.73	2.93	3.58	0.89	10.227	9.794	126
NGC4308	2.00	0.207	3.01	2.29	2.50	2.39	2.69				88
NGC4458	1.91	0.247	4.03	2.18	2.18	2.18	2.96	0.92	10.170	9.429	106
NGC4489	2.16	0.221	2.96	2.97	2.94	2.95	2.96				49
NGC4841B	2.01	0.288	4.80	3.16	3.54	3.35	4.01	0.94	11.485	10.755	229
NGC4926	2.10	0.299	4.82	3.22	1.95	2.59	3.53	0.96	11.417	10.578	270
NGC6086	1.93	0.310	4.87	3.30	2.71	3.01	3.83	0.93	11.936	10.965	304
NGC7454	2.09	0.204	3.24	2.56	2.12	2.34	2.75	0.88	10.512	10.184	103
Galaxies with unusually low [MgFe]											
RR62	1.15	0.130	2.30	1.57	1.82	1.69	1.97				81
RR317b	2.33	0.130	1.82	2.47	1.74	2.10	1.95				91
NGC3156	4.23	0.115	1.81	1.94	1.66	1.80	1.80	0.72	10.104	9.792	112

a review of the subject). In brief, α -elements are mainly ejected by Type II together with some Fe, whereas Fe is essentially expelled by Type Ia supernovae (via the carbon ignition in binary White Dwarfs reaching the Chandrasekhar limit by mass accretion). As long as Type Ia supernovae do not intervene in a significant manner, the chemical composition of the gas and newly formed stars in turn will be enhanced in α -elements. Since Type Ia supernovae are expected to start contaminating the intergalactic medium than Type II (Greggio & Renzini 1983), in the framework of the standard supernova driven galactic wind model by Larson (1974) and the standard initial mass function, the time scale of star formation and galactic wind must be shorter than about 0.5 Gyr not to decrease the initial $[\alpha/Fe] > 0$ (when α -elements are mostly produced) to $[\alpha/Fe] \leq 0$ (when iron is predominantly ejected). In other words, to reproduce the observed trend of the $[\alpha/Fe]$ -mass relationship, the total duration of the star forming activity ought to scale with the galaxy mass according to $\Delta t_{SF} \propto M_G^{-1}$. This is the main drawback of the standard model because it requires a mass-star-formation-timescale correlation which is the opposite of what implied by the Color-Magnitude relationship (Bower et al. 1992a) as amply discussed in Bressan et al. (1996); Chiosi (2000); Chiosi & Carraro (2002) and Tantalo & Chiosi (2002). This point of difficulty has been overcome by the N-Body Tree-SPH model of Chiosi & Carraro (2002). In brief (i) Independently of the total mass, galaxies of high initial density

undergo a prominent initial episode of star formation followed by quiescence. (ii) The same applies to high mass galaxies of low initial density whereas the low mass ones undergo a series of burst-like episodes that may stretch over a considerable fraction of their lifetime. (iii) The mean and maximum metallicity increase with the galaxy mass. Therefore these models can account for the CMR of EGs. (iv) Finally, the occurrence of galactic winds does not follow the simple Larson (1974) model, but takes place continuously in lumps of gas as soon as their thermal kinetic energy exceeds the gravitational energy of the galaxy. In other words the scheme on which the Larson (1974) model rests, i.e. – longer star formation period – higher metallicity – lower degree of α -enhancement at increasing galaxy mass, is reversed but for the metallicity. Therefore the CMR and α -enhancement constraints are met at the same time. See Chiosi & Carraro (2002) and Tantalo & Chiosi (2002) for all details. Given these premises, the existence of various degrees of α -enhancement in different EGs finds a natural explanation thanks to the sensitivity of the star forming process and its duration to the initial conditions (mean density) and total mass of the proto-galaxy. By the same token we may also explain the systematic higher abundance ratios $[\alpha/Fe]$ passing from field to cluster galaxies.

7 WHAT IS THE MAXIMUM COLOR DISPERSION OF EG'S?

Our aim here is to check at what extent a past episode of star formation would reflect on to broad-band colors, such as $(B-V)$, of the host galaxy as we see it today³. To this aim we adapt the toy model of galaxy formation we have been using in so far. The analysis below applies both to the monolithic (isolation) and hierarchical scheme.

For the sake of simplicity let adopt a model with the minimum number of parameters: solar scaled abundances, fixed age for the old stellar component, here indicated as $T_F \simeq 12$ Gyr, fixed mean metallicity. With no further stellar activity, passive evolution of the galaxy would imply that at the present time $(B-V) \simeq 1.00 \pm 0.05$ whereby the uncertainty reflects the spread in metallicity and abundance ratios.

Now suppose that at a certain age T_B the model galaxy undergoes an additional episode of star formation of short duration and arbitrary intensity β_2 (this immediately fixes also the intensity β_1 of the old component, their sum being equal to unity). The burst can be of internal origin (e.g. gas left over by the previous activity and then turned into stars) or the result of a merger with some gas-rich object. In the first case, the galaxy will be made by an old and a young component. In the second case, the galaxy will consist of two sub-units harboring old populations (in principle of different age and metal content) plus the younger component born during the burst.

The color evolution of the composite galaxy is followed up to the present time and its broad-band colors are tested against observations. The results are displayed in the large panel of Fig. 11 as a function of the age and intensity of the secondary activity. Let us now read off the age T_R , at which a galaxy which underwent a burst of star formation of intensity β_2 at the age T_B , is able to recover the same color it had before the burst. This is simply given by the intersection of any line labelled β_2 with the horizontal bar. The ages T_R as function of the β_2 are shown in the small panel of Fig. 11. It turns out that for many combinations of T_B and β_2 , the resulting $(B-V)$ color would be too blue as compared to the typical colors of EG's, $(B-V) = 1.00 \pm 0.05$. Stellar activities engaging 5-10% of the total mass and taking place as early as 5-6 Gyr ago would be detectable. The situation gets even worse for higher β_2 and/or lower T_B . *This implies that only remote or minute star forming events are allowed. Therefore, either mergers occur very early on in a galaxy's history or only captures of small bodies and little companion star formation can take place at later epochs.* This is a rather strong constraint that should be taken into account by any model of hierarchical assembling of big galaxies. It is plausible to suggest that the main body of a galaxy was assembled early on and that all subsequent activity we infer from the observational data is limited to the capture of small objects (likely satellites of the dominant galaxy).

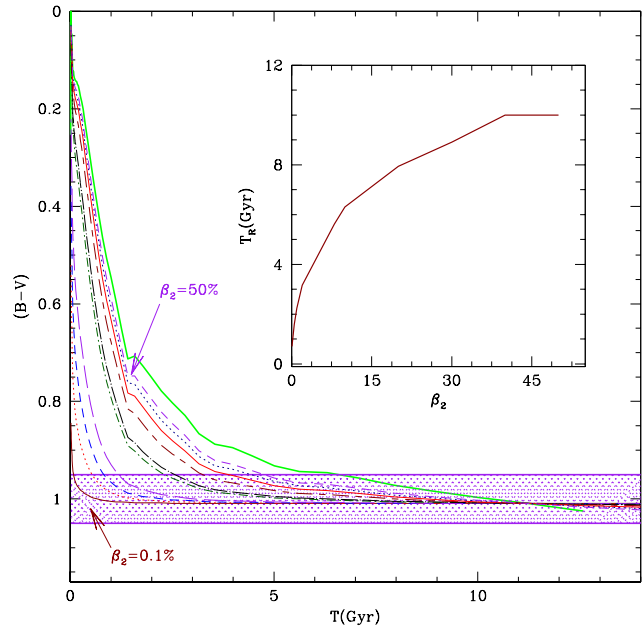


Figure 11. Simulations of the $(B-V)$ color of EGs in which a burst of star formation of arbitrary intensity and age T_B is superposed to an old population with the age of 13 Gyr. In these simulations for both components we assume $Z=0.019$ and $\Gamma=0$. The burst intensity is $\beta_2=0.001, 0.002, 0.005, 0.01, 0.02, 0.08, 0.10, 0.20, 0.30, 0.40,$ and 0.50 , going from bottom-left to top-right as indicated. The horizontal bar visualizes the typical color of EGs with the uncertainty $\Delta(B-V) = \pm 0.055$. The insert shows the time T_R in Gyr elapsed from the epoch of the burst to the stage at which the composite galaxy recovers the typical red colors of EGs as a function of the burst intensity. T_R is given by the intersection of each color curve with the horizontal bar.

8 SUMMARY AND CONCLUDING REMARKS

The present-day challenge with EGs is to unravel their formation and evolution history. In a simplified picture of the issue, the problem can be cast as follows. Do EGs form by hierarchical merging of pre-existing sub-structures (maybe disc galaxies) made of stars and gas? Was each merging event accompanied by strong star formation? Or conversely, they originate from the early aggregation of lumps of gas turned into stars in the remote past via a burst-like episode ever since followed by quiescence so as to mimic a sort of monolithic process? Even if the two alternatives seem to oppose each other, actually they may concur to shaping the final properties of EGs as seen today. The question is to unravel the signature of the forming mechanism from the observational data. To this aim we have examined the line absorption indices on the Lick system of normal, field EGs of Trager (1997) and of interacting EGs (pair- and shell-objects) of Longhetti et al. (2000). Occasionally we have also looked at the EGs in the Coma Clusters of Jørgensen (1999) and other more specific cases taken from literature. The bottom line of this study was (i) to check whether normal (quiescent) and interacting have a different behavior in the popular diagnostic planes such as H_β vs. $[MgFe]$ (and others); (ii) to seek whether the signature of interaction may mirror in some specific changes of the indices that could unequivocally hint

³ Preliminary studies of the same subject are by Chiosi (2000) and Chiosi & Carraro (2002)

for bursts of stellar activity; (iii) to evaluate the intensity of those bursts or secondary episodes of star formation; (iv) to explore whether other alternatives can exist, i.e. distinct from obvious ones resting on large age range and/or bursts of star formation (from one to several) at various epochs.

From the various observational issues we have been examining in so far, we gather the following picture:

(1) Both normal, field and interacting galaxies have the same scattered distribution in the H_β vs. $[MgFe]$ diagnostic plane even the interacting ones show a more pronounced tail toward high H_β values. This may suggest that a common physical cause is at origin of their distribution.

(2) The distribution of normal and interacting galaxies is smoothly elongated in H_β . While for the interacting objects an easy, however not fully satisfactory, explanation can be found invoking a late burst of activity, in the case of normal galaxies an explanation can be found only invoking a large age range for the bulk population together with the existence of an universal law of metal enrichment. Adding a late burst of star formation to an old system without invoking the large age range and the universal law of chemical enrichment would not yield the desired trend. Therefore not only normal galaxies have to be build up over a large time interval but also at increasing total metallicity. The occurrence of late star forming episode is a sort of optional.

(3) More specifically, a typical model based on classical SSPs with solar partition of elements and where the burst is superimposed to an old and coeval population is not able to reproduce the smooth distribution of galaxies in the H_β vs. $[MgFe]$ plane. This kind of model would predict an outstanding clump at low H_β values, contrary to what is observed. Models in which star formation lasted for a significant fraction of the Hubble time ($4 \text{ Gyr} \leq t_{old} \leq 16 \text{ Gyr}$) better match the observed diagram. In this context, the peculiar, almost *vertical* distribution of galaxies (normal, shell- and pair-objects) in the H_β vs. $[MgFe]$ plane is interpreted as the trace of the increase of the *average* metallicity accompanying all star forming events. This could be the signature of a metal enrichment happening on a cosmic scale.

(4) However, the above scheme is firstly too demanding because of the many *ad hoc* ingredients that have to be introduced, secondly it neglects important effects given by the observationally grounded hint that the stellar content of EGs is likely enhanced in α -elements with Γ ranging from 0.1 to 0.4 dex. We would like to propose a new scheme, in which the bulk dispersion of galaxies in the H_β vs. $[MgFe]$ plane is caused by a different mean degree of enhancement. Indeed two old galaxies of the same age (say 13 Gyr) but different Γ and $[X_{el}/Fe]$ for some important species (C,N,O... Ti) would have different values of H_β . For instance passing from a 13 Gyr old galaxy with $\Gamma=0$ to an object with the same age but $\Gamma=0.3$ would increase H_β by as much as 0.2-0.3 or more (depending on the abundance ratios for some specific elements like Ti). The effect is comparable to the mean observational dispersion. The majority of EGs can be pretty old (10-13 Gyr). Furthermore, neither large age range nor universal enrichment law are required. The *nearly vertical* smooth distribution for coeval galaxies is secured by the compensatory effect of different combinations of Z and Γ . Finally, the occurrence of a late burst of activity is not an un-avoidable ingredient of the recipe, but a rare event interesting only those galaxies with very high H_β (roughly

> 2.5). The possibility that EGs span large ranges of Γ and metallicities but narrow ranges of ages for the bulk population favors the monolithic scheme and can be derived from N-Body Tree-SPH models of galaxy formation as a consequence of the dependence of the star formation efficiency and temporal history on the initial mean density and total mass of the proto-galaxy.

(5) As far as we can tell, from simulations of broad-band colors, EGs are compatible with the notion that the bulk stars have formed in the remote past. Galaxy mergers and companion star formation in a recent past are not likely, unless the intensity of the secondary activity is very small (i.e. engaging less than a few percent of the total mass). Were merging the only possible mechanism to form massive EGs, this should have occurred in a remote past (half of the Hubble time at least). In any case merging of smaller units without star formation even in a recent past cannot be excluded. Is it likely?

(6) Finally, prolonged or secondary stellar activity seem to be also more probable in field and loose groups EGs than in those belonging to compact groups and clusters. The physical cause could once more be the mean density of the environment out of which proto-galaxies are formed.

ACKNOWLEDGEMENTS

This study has been financed by the Italian Ministry of Education, University, and Research (MIUR), and the University of Padua under the special contract "Formation and evolution of elliptical galaxies: the age problem".

REFERENCES

- Allard F., Hauschildt P., Tamanai A., Ferguson J., 2000, in Griffith C., Marley M., eds, ASP Conf. Ser. 212: From Giant Planets to Cool Stars Model atmospheres and spectra of brown dwarfs to giant planets. p. 127
- Balcells M., Peletier R. F., 1994, AJ, 107, 135
- Bertelli G., Bressan A., Chiosi C., Fagotto F., Nasi E., 1994, A&AS, 106, 275
- Bertola F., Burstein D., Buson L. M., 1993, ApJ, 403, 573
- Bessell M., Castelli F., Plez B., 1998, A&A, 333, 231
- Bessell M. S., 1990, PASP, 102, 1181
- Bessell M. S., Brett J. M., 1988, PASP, 100, 1134
- Bower R. G., Kodama T., Terlevich A., 1998, MNRAS, 299, 1193
- Bower R. G., Lucey J. R., Ellis R. S., 1992a, MNRAS, 254, 589
- Bower R. G., Lucey J. R., Ellis R. S., 1992b, MNRAS, 254, 601
- Bressan A., Chiosi C., Fagotto F., 1994, ApJS, 94, 63
- Bressan A., Chiosi C., Tantalo R., 1996, A&A, 311, 425
- Burstein D., Bender R., Faber S., Nolthenius R., 1997, AJ, 114, 1365
- Burstein D., Bertola F., Buson L. M., Faber S. M., Lauer T. R., 1988, ApJ, 328, 440
- Burstein D., Faber S. M., Gaskell C. M., Krumm N., 1984, ApJ, 287, 586
- Buson L., Bertola F., Burstein D., Cappellari M., 2004, private communication

- Buzzoni A., Gariboldi G., Mantegazza L., 1992, *AJ*, 103, 1814
- Buzzoni A., Mantegazza L., Gariboldi G., 1994, *AJ*, 107, 513
- Carollo C. M., Danziger I. J., 1994a, *MNRAS*, 270, 523
- Carollo C. M., Danziger I. J., 1994b, *MNRAS*, 270, 743
- Carollo C. M., Danziger I. J., Buson L., 1993, *MNRAS*, 265, 553
- Carrasco L., Buzzoni A., Salsa M., Recillas-Cruz E., 1995, in Buzzoni A., Renzini A., Serrano A., eds, *ASP Conf. Ser. 86: Fresh Views of Elliptical Galaxies* p. 235
- Castelli F., Gratton R., Kurucz R., 1997, *A&A*, 318, 841
- Chiosi C., 2000, in Hubney I., Heap S. R., Cornett R. H., eds, *Spectro-photometric Dating of Stars and Galaxies* Vol. 192 of *ASP Conf. Ser.* p. 251
- Chiosi C., Carraro G., 2002, *MNRAS*, 335, 335
- Davies R. L., Kuntschner H., Emsellem E., Bacon R., Bureau M., Carollo C. M., Copin Y., Miller B. W., Monnet G., Peletier R. F., Verolme E. K., de Zeeuw P. T., 2001, *ApJL*, 548, L33
- Davies R. L., Sadler E. M., Peletier R. F., 1993, *MNRAS*, 262, 650
- Ellis R., 1998, *Nature*, 395, A3
- Faber S. M., Friel E. D., Burstein D., Gaskell C. M., 1985, *ApJS*, 57, 711
- Faber S. M., Worthey G., González J. J., 1992, in Barbuy B., Renzini A., eds, *The Stellar Population of Galaxies* IAU Symp. 149. Kluwer Academic Publishers: Dordrecht, p. 255
- Fisher D., Franx M., Illingworth G., 1995, *ApJ*, 448, 119
- Fisher D., Franx M., Illingworth G., 1996, *ApJ*, 459, 110
- Fluks M. A., Plez B., Thé P. S., de Winter D., Westerlund B., Steenman H., 1994, *A&AS*, 105, 311
- Freedman W. L., 1989, *AJ*, 98, 1285
- Freedman W. L., 1992, *AJ*, 104, 1349
- Girardi L., Bertelli G., 1998, *MNRAS*, 300, 533
- Girardi L., Bertelli G., Bressan A., Chiosi C., Groenewegen M., Marigo P., Salasnich B., Weiss A., 2002, *A&A*, 391, 195
- Girardi L., Bressan A., Bertelli G., Chiosi C., 2000, *A&AS*, 141, 371
- González J. J., 1993, PhD thesis, University of California, Santa Cruz
- Gorgas J., Faber S. M., Burstein D., González J. J., Courteau S., Prosser C., 1993, *ApJS*, 86, 153
- Gratton R., Carretta E., Claudi R., Lucatello S., Barbieri M., 2003, *A&A*, 404, 187
- Greggio L., 1996, *MNRAS*, 285, 151
- Greggio L., Renzini A., 1983, *A&A*, 118, 217
- Grillmair C. J., Lauer T. R., Worthey G., Faber S. M., Freedman W. L., Madore B. F., Ajhar E. A., Baum W. A., Holtzman J. A., Lynds C. R., O'Neil E. J., Stetson P. B., 1996, *AJ*, 112, 1975
- Hamabe M., Kormendy J., 1987, in de Zeeuw T., ed., *IAU Symp. 127: Structure and Dynamics of Elliptical Galaxies* p. 379
- Jørgensen I., 1997, *MNRAS*, 288, 161
- Jørgensen I., 1999, *MNRAS*, 306, 607
- Kawata D., 1999, *Publ. Astron. Soc. Jpn.*, 51, 931
- Kawata D., 2001a, *ApJ*, 558, 598
- Kawata D., 2001b, *ApJ*, 548, 703
- Kuntschner H., 1998, PhD thesis, Univ. of Durham
- Kuntschner H., 2000, *MNRAS*, 315, 184
- Kuntschner H., Davies R. L., 1998, *MNRAS*, 295, L29
- Kuntschner H., Lucey J. R., Smith R. J., Hudson M. J., Davies R. L., 2001, *MNRAS*, 323, 615
- Larson R. B., 1974, *MNRAS*, 142, 501
- Leonardi A. J., Worthey G., 2000, *ApJ*, 534, 650
- Longhetti M., Bressan A., Chiosi C., Rampazzo R., 1999, *A&A*, 345, 419
- Longhetti M., Bressan A., Chiosi C., Rampazzo R., 2000, *A&A*, 353, 917
- Longhetti M., Rampazzo R., Bressan A., Chiosi C., 1998a, *A&AS*, 130, 251
- Longhetti M., Rampazzo R., Bressan A., Chiosi C., 1998b, *A&AS*, 130, 267
- Maraston C., Greggio L., Renzini A., S.Ortolani Saglia R., Puzia T., Kissler-Patig M., 2003, *A&A*, 400, 823
- Matteucci F., 1994, *A&A*, 288, 57
- Matteucci F., 1997, *Fundam. Cosmic Phys.*, 17, 283
- Matteucci F., Ponzzone R., Gibson B. K., 1998, *A&A*, 335, 855
- Mehlert D., Thomas D., Saglia R., Bender R., Wegner G., 2003, *A&A*, 407, 423
- Peebles P., 2002, in Metcalfe N., Shanks T., eds, *ASP Conf. Ser. 283: A New Era in Cosmology* p. 351
- Poggianti B., Bridges T., Mobasher B., Carter D., Doi M., Iye M., Kashikawa N., Komiyama Y., Okamura S., Sekiguchi M., Shimasaku K., Yagi M., Yasuda N., 2001, *ApJ*, 562, 689
- Reimers D., 1975, *Mem. Soc. R. Sci. Liege*, ser. 6, 8, 369
- Renzini A., Buzzoni A., 1986, in Chiosi C., Renzini A., eds, *Spectral Evolution of Galaxies* Dordrecht: Reidel, p. 213
- Ryan S., Norris J., Bessell M., 1991, *AJ*, 102, 303
- Salasnich B., Girardi L., Weiss A., Chiosi C., 2000, *A&A*, 361, 1023
- Tantalo R., 1998, PhD thesis, Univ. of Padova
- Tantalo R., Chiosi C., 2002, *A&A*, 388, 396
- Tantalo R., Chiosi C., 2004, *MNRAS*, submitted
- Tantalo R., Chiosi C., Bressan A., 1998, *A&A*, 333, 419
- Tantalo R., Chiosi C., Bressan A., Marigo P., Portinari L., 1998, *A&A*, 335, 823
- Tantalo R., Chiosi C., Munari U., Piovani L., Sordo R., 2004, *MNRAS*, submitted
- Thomas D., Maraston C., 2003, *A&A*, 401, 429
- Thomas D., Maraston C., Bender R., 2003a, *MNRAS*, 339, 897
- Thomas D., Maraston C., Bender R., 2003b, *MNRAS*, 343, 279
- Trager S., 1997, PhD thesis, Univ. of California, Santa Cruz
- Trager S. C., Faber S. M., Worthey G., González J. J., 2000a, *AJ*, 120, 165
- Trager S. C., Faber S. M., Worthey G., González J. J., 2000b, *AJ*, 119, 1645
- Tripicco M. J., Bell R. A., 1995, *AJ*, 110, 3035
- Vassiliadis D. A., Wood P. R., 1993, *ApJ*, 413, 641
- Vazdekis A., Kuntschner H., Davies R. L., Arimoto N., Nakamura O., Peletier R. F., 2001, *apj*, 551, 127
- Worthey G., 1992, PhD thesis, Univ. of California
- Worthey G., Faber S. M., González J. J., Burstein D., 1994, *ApJS*, 94, 687